

Critical Theory of the Two-Channel Anderson Impurity Model

Henrik Johannesson

*Institute of Theoretical Physics,
Chalmers University of Technology and Göteborg University,
SE-412 96 Göteborg, Sweden*

N. Andrei and C. J. Bolech*

*Center for Materials Theory,
Serin Physics Laboratory, Rutgers University
Piscataway, New Jersey 08854-8019*

We construct the boundary conformal field theory that describes the low-temperature behavior of the two-channel Anderson impurity model. The presence of an exactly marginal operator is shown to generate a line of stable fixed points parameterized by the charge valence n_c of the impurity. We calculate the exact zero-temperature entropy and impurity thermodynamics along the fixed line. We also derive the critical exponents of the characteristic Fermi edge singularities caused by time-dependent hybridization between conduction electrons and impurity. Our results suggest that in the mixed-valent regime ($n_c \neq 0, 1$) the electrons participate in two competing processes, leading to frustrated screening of spin *and* channel degrees of freedom. By combining the boundary conformal field theory with the Bethe Ansatz solution we obtain a complete description of the low-energy dynamics of the model.

PACS numbers: 71.27.+a, 75.20.Hr, 75.40.-s

I. INTRODUCTION

In recent years, a growing class of materials has been shown to exhibit metallic behaviors that violate Landau's Fermi liquid theory.¹ Examples include the "normal phases" of underdoped and optimally doped high- T_c cuprates,² a variety of (quasi) one-dimensional conductors – ranging from single-wall carbon nanotubes³ to the Bechgaard salts⁴ – several artificially designed nanostructures,⁵ as well as certain cerium- and uranium-based heavy fermion alloys.⁶ In light of the spectacular success of Landau's theory in explaining the properties of conventional metals, the proliferation of experimental systems that depart from its predictions presents a challenge to the theorist. Not forming a Fermi liquid, the mobile electrons of these systems cannot be adiabatically connected to a noninteracting electron gas, and their description requires a theoretical approach of a different brand.

A particularly intriguing case is that of the heavy fermion compound UBe_{13} . Like several other metallic materials containing rare earth or actinide ions with partially filled f-electron shells UBe_{13} exhibits manifest non-Fermi liquid behavior at low temperatures. In particular, the specific heat shows a $T \ln T$ behavior all the way down to the superconducting transition (at roughly 1K),⁷ suggestive of a two-channel overscreened Kondo effect driven by the f-electrons of the uranium ions. There are two possible integer valence configurations for uranium embedded in a Be_{13} host: a Γ_6 magnetic spin doublet in the $5f^3$ configuration and a Γ_3 electrical quadrupolar doublet in the $5f^2$ configuration, the two levels being separated by an energy ε . Arguing that the extremely weak magnetic field dependence of the material⁶ excludes

the usual magnetic Kondo effect, Cox⁸ proposed that the observed anomalies instead derive from a quenching of the quadrupolar degrees of freedom by the local orbital motion of the Γ_8 conduction electrons in the material (with the electron spin $\sigma = \uparrow, \downarrow$ providing the two "channels" required for overscreening). The proposal has been controversial,⁹ however, and experimental data on the nonlinear magnetic susceptibility indicate that the low-lying magnetic excitations are rather predominantly dipolar in character.¹⁰ Whether the energy splitting ε between the two doublets is sufficiently large for a quadrupolar Kondo scenario to become viable is an additional unresolved issue. Aliev *et al.*¹¹ have suggested that the magnetic and quadrupolar doublets may in fact be near degenerate, leading instead to a mixed-valent state with a novel type of interplay between quadrupolar and magnetic Kondo-type screening. Indirect support for this hypothesis comes from non-linear susceptibility¹¹ and other¹² measurements on the thoriated compound $\text{U}_{0.9}\text{Th}_{0.1}\text{Be}_{13}$. The presence of thorium ions suppresses the superconducting transition in the undoped material and one observes instead a crossover from a magnetic to a quadrupolar groundstate at low temperatures.

The simplest model that captures a possible mixed-valent regime with both magnetic and quadrupolar character is the two-channel Anderson single-impurity model.^{13,14,15} In this model the conduction electrons carry both spin ($\sigma = \uparrow, \downarrow$) and quadrupolar ($\alpha = \pm$) quantum numbers, and hybridize via a matrix element V with a local uranium ion. The ion is modeled by a quadrupolar ($5f^2$) doublet created by a boson operator b_α^\dagger and a magnetic ($5f^3$) doublet created by a fermion operator f_σ^\dagger . Strong Coulomb repulsion implies that the localized f-levels can carry at most one electron, and this condition

is implemented as an operator identity for the pseudoparticles: $f_\sigma^\dagger f_\sigma + b_{\bar{\alpha}}^\dagger b_{\bar{\alpha}} = 1$, where $\bar{\alpha}$ denotes the conjugate representation. With these provisos the Hamiltonian is written as

$$H = H_{bulk} + H_{ion} + H_{hybr}, \quad (1)$$

where

$$H_{bulk} = \int dx : \psi_{\alpha\sigma}^\dagger(x) (-i\partial_x) \psi_{\alpha\sigma}(x) : \quad (2)$$

$$H_{ion} = \varepsilon_s f_\sigma^\dagger f_\sigma + \varepsilon_q b_{\bar{\alpha}}^\dagger b_{\bar{\alpha}} \quad (3)$$

$$H_{hybr} = V[\psi_{\alpha\sigma}^\dagger(0) b_{\bar{\alpha}}^\dagger f_\sigma + f_\sigma^\dagger b_{\bar{\alpha}} \psi_{\alpha\sigma}(0)]. \quad (4)$$

Here the conduction electrons are described by one-dimensional fields $\psi_{\alpha\sigma}^\dagger(x)$, matching the Γ_8 representation (appearing in the reduction of $\Gamma_3 \times \Gamma_6$ and thus coupling to the impurity). The electron fields are chiral, obtained - as usual¹⁶ - by reflecting the outgoing radial ($x > 0$), Γ_8 -component of the original three-dimensional problem to the negative x -axis and disregarding components that do not couple to the ion at $x = 0$. The spectrum is linearized around the Fermi level and the Fermi velocity is set to unity, with the resulting density of states being $\rho = 1/(2\pi)$. The normal ordering is taken with respect to the filled Fermi sea, and the energies ε_s and ε_q are those of the magnetic and quadrupolar doublets respectively.

Recently two of us presented an exact solution of the model, based on a Bethe Ansatz construction.¹⁷ A complete determination of the energy spectrum and the thermodynamics was given, allowing a full description of the evolution of the impurity from its high temperature behavior with all four impurity states being equally populated down to the low energy dynamics characterized by a line of fixed point Hamiltonians $H^*(\varepsilon, \Gamma)$ where $\varepsilon = \varepsilon_s - \varepsilon_q$ and $\Gamma = \pi\rho V^2$ (Γ is held fixed in what follows).

It is found that the line of fixed points is characterized by a zero-temperature entropy $S_{\text{imp}}^0 = k_B \ln \sqrt{2}$ and a specific heat $C_v^{\text{imp}} \sim T \ln T$ typical of the two-channel Kondo fixed point. However, the physics along the line varies with ε . Consider $n_c = \langle f_\sigma^\dagger f_\sigma \rangle$, the amount of charge localized at the impurity. For $\varepsilon \lesssim \mu - \Gamma$, one finds that $n_c \approx 1$, signaling the magnetic integral valence regime. At intermediate temperatures a magnetic moment forms which undergoes frustrated screening as the temperature is lowered, leading to zero-temperature anomalous entropy and anomalous specific heat. For $\varepsilon \gtrsim \mu + \Gamma$ the system is in the quadrupolar integral regime and a quadrupolar moment forms. In the mixed valence regime, $|\varepsilon - \mu| \lesssim \Gamma$, similar low-temperature behavior is observed though without the intermediate regime of moment formation. In more detail, each point on the line of fixed points is characterized by two energy scales $T_{l,h}(\varepsilon)$. These scales describe the quenching of the entropy as the temperature is lowered: the first stage taking place at the high-temperature scale T_h , quenching the entropy from

$k_B \ln 4$ to $k_B \ln 2$, the second stage at T_l , quenching it from $k_B \ln 2$ to $k_B \ln \sqrt{2}$. In the integral valence regime, $|\varepsilon - \mu| \gg \Gamma$, the two scales are well separated and as long as the temperature falls between these values a moment is present (magnetic or quadrupolar depending on the sign of $\varepsilon - \mu$), manifested by a finite temperature plateau $S_{\text{imp}} = k_B \ln 2$ in the entropy. It is quenched when the temperature is lowered below T_l , with $T_l \rightarrow T_K$ in this regime. For $\varepsilon = \mu$ the scales are equal, $T_l(\mu) = T_h(\mu)$, and the quenching occurs in a single stage.

In the present paper we shall concentrate on the low-energy regime and give a detailed description of the line of fixed points in terms of boundary conformal field theory - the low-energy effective Hamiltonian. It was argued by Affleck and Ludwig^{18,19} that the low-energy regime of a quantum impurity problem is described by a boundary conformal field theory (BCFT) with a conformally invariant boundary condition replacing the dynamical impurity. However, to identify the effective low-energy theory characterizing a given microscopic impurity model, such as Hamiltonian (1), it is necessary to employ more powerful methods, valid over the full energy range, that can connect the microscopic Hamiltonian to the effective low-energy theory. One needs in principle to carry out a full renormalization group calculation or, when available, use an exact solution to extract the BCFT.

Although applicable only in the neighborhood of a low-temperature fixed point, a BCFT formulation has certain advantages. First, it provides an elegant scheme in which to analyze the approach to criticality. The leading scaling operators can be identified explicitly, yielding access to the low-temperature thermodynamics in closed analytical form. These can be matched with the expressions from the Bethe-Ansatz solution allowing the determination of the parameters appearing in the BCFT. This will be carried out below. Secondly - and more importantly - having identified the scaling operators, the asymptotic dynamical properties (Green's functions, resistivities, optical conductivities, etc.) can in principle be calculated. These results will be presented in a subsequent work.

The paper is organized as follows. In Sec. II we review the basics of BCFT, with particular focus on applications to quantum impurity problems. In Sec. III we derive the specific BCFT which describes the low-temperature physics of the two-channel Anderson model in Eq. (1). Some important features of this BCFT are discussed, and in this section we also apply it to the Fermi edge singularity problem for this model. In Sec. IV we then combine the results obtained with the Bethe Ansatz solution¹⁷ to analytically calculate the zero-temperature impurity entropy, the impurity contributions to the low-temperature specific heat, and the linear and non-linear impurity magnetic susceptibilities. Section V, finally, contains a summary and a discussion of our results.

II. BOUNDARY CONFORMAL FIELD THEORY APPROACH

The BCFT approach to quantum impurity problems is well reviewed in the literature,^{20,21,22} and we here only collect some basic results so as to fix conventions and notation.

The key idea is to trade a local impurity-electron interaction for a scale invariant boundary condition on the critical theory that represents the extended (electron) degrees of freedom. In the presence of a boundary, the left- and right-moving parts of the fields $\varphi(t, x)$ in the critical theory are identified via analytic continuation beyond the boundary $x = 0$, such that

$$\varphi(t, x) = \varphi_L(t, x)\varphi_R(t, x) \rightarrow \varphi_L(t, x)\varphi_L(t, -x). \quad (5)$$

Thus, the boundary effectively turns the fields nonlocal. The consequence of this can be delineated via the operator product expansion

$$\varphi_L(z)\varphi_L(z^*) \rightarrow \sum_j \frac{g_j}{(z - z^*)^{2\Delta - \Delta_j}} \mathcal{O}_L^{(j)}(0, \tau), \quad z \rightarrow z^*. \quad (6)$$

We have here introduced a complex variable $z = \tau + ix$, with τ the Euclidean time and x the spatial coordinate. The function g_j ($= 0$ or 1) selects the *boundary operators* $\mathcal{O}_L^{(j)}$ associated with the given boundary condition, Δ_j (Δ) being the dimension of $\mathcal{O}_L^{(j)}$ (φ_L). It follows from Eqs. (5) and (6) that an n -point function of a field φ close to the boundary turns into a linear combination of n -point functions of the *chiral* boundary operators $\mathcal{O}_L^{(j)}$. In particular, this implies that the *boundary scaling dimension* Δ_{bound} of φ that governs its autocorrelation function close to the boundary,

$$\langle \varphi(t, x)\varphi(0, x) \rangle - \langle \varphi(t, x) \rangle \langle \varphi(0, x) \rangle \sim t^{-2\Delta_{\text{bound}}} |t| \gg |x| \quad (7)$$

is precisely given by the scaling dimension of the *leading* boundary operator appearing in Eq. (6).

This sets the strategy for treating a quantum impurity problem: identify first the particular boundary condition that plays the role of the impurity interaction. Given that this boundary condition is indeed scale invariant (together with the original bulk theory), one can then use the machinery of BCFT to extract the corresponding boundary scaling dimensions. As these determine the asymptotic autocorrelation functions [cf. Eq. (7)] the finite-temperature properties due to the presence of the boundary (*alias* the impurity) are easily accessed from standard finite-size scaling by treating the (Euclidean) time as an inverse temperature.

To identify the “right” boundary condition it is convenient to exploit a well-known result²³ from conformal

field theory, relating the energy levels in a finite geometry to the (boundary) scaling dimensions of operators in the (semi-) infinite plane. More precisely, consider a conformally invariant theory defined on the strip $\{w = u + iv \mid -\infty < u < \infty, 0 \leq v \leq \ell\}$ with u the Euclidean time and v the space coordinate. Then impose a conformally invariant boundary condition, call it A , at the edges $v = 0$ and $v = \ell$, and map the strip onto the semi-infinite plane $\{z = \tau + ix \mid x \geq 0\}$ using the conformal transformation $z = \exp(\pi w/\ell)$ (implying boundary condition A at $x = 0$). With E_0 the ground-state energy, one has

$$E_n = E_0 + \frac{\pi \Delta_n}{\ell}, \quad (8)$$

where $\{E_n\}$ is the spectrum of excited energy levels in $0 \leq v \leq \ell$ and $\{\Delta_n\}$ is the spectrum of *boundary scaling dimensions* in the semi-infinite plane.

The problem is thus reduced to determining the finite-size spectrum of the theory. In certain privileged cases this can be done by direct calculation. Alternatively, one hypothesizes a boundary condition and compares the consequences with known answers. An example is the *fusion hypothesis* of Affleck and Ludwig.¹⁹ One here starts with some known, trivial boundary condition on the critical theory, with no coupling to the impurity. For free electrons carrying charge, spin (and maybe some additional “flavor” degrees of freedom) the spectrum organizes into a conformal tower structure,²⁴ with the charge, spin and flavor sectors “glued” together so as to correctly represent the electrons (*Fermi liquid gluing condition*). Then, turning on the electron-impurity interaction, its only effect – according to the fusion hypothesis – is to replace this gluing condition by some new nontrivial gluing of the conformal towers. In the case of the m -channel Kondo problem, the new gluing condition is obtained via *Kac-Moody fusion*²⁵ with the spin-1/2 primary operator that “corresponds” to the Kondo impurity. As a consequence, the conformal tower with spin quantum number j_s is mapped onto new towers labeled by j'_s , where $j'_s = |j_s - \frac{1}{2}|, |j_s - \frac{1}{2}| + 1, \dots, \min\{j_s + \frac{1}{2}, m - j_s - \frac{1}{2}\}$. This is the essence of the BCFT approach, as applied to the Kondo problem.

For the two-channel Anderson model in Eq. (1) it is *a priori* less obvious which operator to use for fusion. Here we shall instead identify the finite-size spectrum by studying certain known limiting cases, guided by the exact Bethe Ansatz solution of the model.¹⁷ As it turns out, the spectrum thus obtained can be reconstructed by fusion with the leading *flavor* boundary operator (representing the channel, or *quadrupolar*, degrees of freedom), but *in addition there occurs an effective renormalization of the charge sector*. This signals the novel aspect of the present problem. A technical remark may here be appropriate: Since the boundary scaling dimensions in Eq. (8) are connected to energy levels in a strip with the *same* boundary condition at the two edges, we are effectively considering a finite-size energy spectrum with *two* quantum impurities present, one at each edge of the strip.

Formally, this can be taken care of by performing Kac-Moody fusion *twice* with the relevant primary operator (*double fusion*). This is an important point, not always fully appreciated in the literature.

Let us finally mention that there exists another, more fundamental description of BCFT,²⁶ based on the notion of *boundary states*, particularly useful when studying zero-temperature properties of a quantum impurity problem. We shall give a brief exposition of it in Sec. (IV.A), where we use it for analyzing the zero-temperature entropy contributed by the impurity.

III. FINITE-SIZE SPECTRUM AND SCALING OPERATORS

As we discussed in the previous section, the scaling dimensions of the boundary operators that govern the critical behavior are in one-to-one correspondence with the levels of the finite-size spectrum of the model. In the present case the spectrum can in principle be constructed from the exact Bethe Ansatz solution in Ref. 17, but this requires an elaborate analysis. The reason is that the solution takes the form of a so called “string solution” even in the groundstate. Since a string solution is valid only in the thermodynamic limit, an application of standard finite-size techniques²⁷ would lead to incorrect results. One may instead pursue another strategy and identify the finite size spectrum (hence the dimensions of the scaling operators) that reproduces the results of the exact solution in the low-energy limit. In our case the search for the wanted spectrum can be carried out efficiently by combining symmetry arguments with known results for the finite-size spectra for two limiting cases of the Hamiltonian (1): the ordinary Anderson model and the two-channel Kondo model. We shall see that the low energy spectrum thus obtained, Eq. (22) below, leads indeed to a line of fixed points characterized by entropy $S = k_B \ln \sqrt{2}$ and susceptibility $C_V \sim T \ln T$ as required by the Bethe Ansatz solution. The fitting of the proposed spectrum to the solution also allows the determination of all thermodynamically relevant parameters in the BCFT.

A. Identifying the Critical Theory

Let us begin by reviewing the single channel Anderson and Kondo models. The latter is obtained in the

integer-valence limit $n_c \rightarrow 1$ (with $n_c \equiv \langle f_\sigma^\dagger f_\sigma \rangle$ measuring the charge localized at the impurity site) where a magnetic moment forms, signaling the entrance to the Kondo regime.²⁸ It is instructive to consider this case in some detail before proceeding to an analysis of the full model in Eq. (1).

As is well known, the ordinary Anderson model²⁹ with integer valence $n_c = 1$ can be mapped onto the single-channel Kondo model via a Schrieffer-Wolff transformation.²⁸ To $O(1/\ell)$, with ℓ the length of the system, the finite-size energy spectrum of the Kondo model takes the form¹⁹

$$E = E_0 + \frac{\pi}{\ell} \left[\left(\frac{1}{4} Q^2 + N_c \right) + \left(\frac{j_s(j_s + 1)}{3} + N_s \right) \right], \quad (9)$$

where the Fermi velocity has been set to unity, as in Eq. (1). Here $Q \in \mathbb{Z}$ and $j_s = 0, 1/2$ are charge and spin quantum numbers – defined with respect to the filled Fermi sea – and labeling the corresponding Kac-Moody *primary states*.²⁵ The positive integers N_c and N_s index the *descendant levels* in the associated $U(1)$ and $SU(2)_1$ conformal towers. The quantum numbers are constrained to appear in the combinations

$$\begin{aligned} Q &= 0 \pmod{2}, & j_s &= \frac{1}{2} \\ Q &= 1 \pmod{2}, & j_s &= 0 \end{aligned} \quad (10)$$

which define the *Kondo gluing conditions* for charge and spin conformal towers.

We can rewrite this result in a form immediately generalizable to the Anderson model, viewing it as the $n_c \rightarrow 1$ limit of the Anderson model spectrum. Redefine the charge quantum number in Eqs. (9) and (10): $Q \rightarrow Q - 1$. The offset mirrors the fact that the Anderson impurity carries charge (in contrast to a Kondo impurity) and, therefore, shifts the net amount of charge in the groundstate compared to the Kondo case. We thus write for the finite-size spectrum of the Anderson model in the $n_c \rightarrow 1$ limit:

$$E = E_0 + \frac{\pi}{\ell} \left[\left(\frac{1}{4} (Q - 1)^2 - \frac{1}{4} + N_c \right) + \left(\frac{j_s(j_s + 1)}{3} + N_s \right) \right], \quad (11)$$

with

$$\begin{aligned} Q &= 0 \pmod{2}, & j_s &= 0 \\ Q &= 1 \pmod{2}, & j_s &= \frac{1}{2} \end{aligned} \quad (12)$$

Note that the constraints in Eqs. (12) are the same as

those for the charge and spin conformal towers of free electrons (*Fermi liquid gluing conditions*). Also note that we have renormalized the groundstate energy, so that $E_0 = E(Q = 0)$, by subtracting off a constant $\pi/4\ell$. The redefinition of charge quantum numbers implies a relabeling of levels: the Q -level in Eq. (9) (constrained by Eqs. (10)) corresponds to the $(Q-1)$ -level in Eq. (11) (with the constraint (12)), modulo the $\pi/4\ell$ shift.

Let us now consider the spectrum of the Anderson model away from the Kondo limit, $n_c \neq 1$. Assuming

$$E = E_0 + \frac{\pi}{\ell} \left[\left(\frac{1}{4}(Q - n_c)^2 - \left(\frac{n_c}{2}\right)^2 + N_c \right) + \left(\frac{j_s(j_s + 1)}{3} + N_s \right) \right], \quad (13)$$

with Q and j_s constrained by Eqs. (12). Note that this result has been extracted from the Kondo finite-size spectrum in Eqs. (9) and (10) simply by keeping track on the offset of charge with respect to the filled Fermi sea as the impurity acquires a nonzero charge valence n_c . The additional assumption that no relevant operator is generated as we move away from the Kondo limit $n_c = 1$ (and that therefore the gluing conditions in Eqs. (10) remain un-

changed), will be shown to be self-consistent when we analyze the full two-channel Anderson model.

We can corroborate our procedure by comparing our result in Eq. (13) with that obtained by Fujimoto and collaborators.³⁰ Applying standard finite-size techniques²⁷ to the exact Bethe Ansatz solution³¹ of the Anderson model these authors found that

$$E = E_0 + \frac{\pi}{\ell} \left[\left(\frac{1}{4}(Q - \frac{2\delta_F}{\pi})^2 - \left(\frac{\delta_F}{\pi}\right)^2 + N_c \right) + \left(\frac{j_s(j_s + 1)}{3} + N_s \right) \right] + O\left(\frac{1}{\ell^2}\right), \quad (14)$$

with Fermi liquid gluing (12) of Q and j_s . The phase shift $\delta_F \equiv \delta_\sigma(\epsilon_F)$ appearing in (14) is that of an electron with spin σ at the Fermi level, related to the average charge $n_c \equiv \langle f_\sigma^\dagger f_\sigma \rangle$ at the impurity site by the Friedel-Langreth sum rule³²

$$\delta_F = \frac{\pi}{2} n_c. \quad (15)$$

Inserting Eq. (15) into Eq. (14), we immediately recover our result (13).

Before returning to the full two-channel Anderson model, let us point out that the duality between the charge shift $Q \leftrightarrow Q-1$ in the integer valence limit $n_c = 1$ and the change of gluing conditions (12) \leftrightarrow (10) simply reflects the well-known fact that the ordinary Kondo effect can formally be described as a local potential scattering of otherwise free electrons, causing a phase shift $\delta_F = \pi/2$ of their wave functions [cf. Eq. (15)]. It is instructive to make this duality transparent by identifying the effective low-energy Hamiltonian H_{charge} that produces the charge spectrum in Eq. (11). Introducing the

charge currents

$$J(x) =: \psi_{\alpha\sigma}^\dagger(x) \psi_{\alpha\sigma}(x): \quad (16)$$

(where as before the normal ordering is taken with respect to the filled Fermi sea), one immediately recognizes the charge part of (11) as the spectrum of the Sugawara Hamiltonian²⁵

$$H_{charge} = \frac{1}{4} \int dx : J(x) J(x) : - \frac{1}{2} J(0). \quad (17)$$

The term $\sim J(0)$ explicitly reveals the presence of an effective local scattering potential. By redefining the charge quantum numbers in the integer valence limit, $Q-1 \rightarrow Q$, this potential is disguised as a renormalized boundary condition, encoded in the Kondo gluing conditions (10).

With these preliminaries let us now go back to the full two-channel Anderson model in Eq. (1), first considering the case when $\varepsilon = \varepsilon_s - \varepsilon_q \ll \mu - \Gamma$. From the Bethe Ansatz solution¹⁷ one finds that in this limit the physics is that of the overscreened two-channel (magnetic) Kondo model.³³ This is expected, since for this case the ion has

integer valence, with an associated magnetic moment of spin $1/2$. The finite-size spectrum of the two-channel Kondo model has been derived from that of free electrons

(carrying spin *and* flavor) via *Kac-Moody fusion*²⁵ with the spin- $1/2$ conformal tower.¹⁹ One finds, to $O(1/\ell)$,

$$E = E_0 + \frac{\pi}{\ell} \left[\left(\frac{1}{8} Q^2 + N_c \right) + \left(\frac{j_s(j_s + 1)}{4} + N_s \right) + \left(\frac{j_f(j_f + 1)}{4} + N_f \right) \right]. \quad (18)$$

Here $Q \in \mathbb{Z}$ are U(1) charge quantum numbers, while $j_{s(f)} = 0, 1/2, 1$ are quantum numbers for the level-2 SU(2) spin (flavor) primary states, with N_c , N_s , and N_f labeling the corresponding descendant levels. The quantum numbers are restricted to appear in the combinations

$$\begin{aligned} Q = 0 \bmod 2, \quad j_s = \frac{1}{2}, \quad j_f = 0 \text{ or } 1, \\ Q = 1 \bmod 2, \quad j_s = 0 \text{ or } 1, \quad j_f = \frac{1}{2}, \end{aligned} \quad (19)$$

which define the *two-channel Kondo gluing conditions*¹⁹ for the conformal towers. Since the charge quantum numbers in Eqs. (19) are defined modulo 2, we can make a shift $Q \rightarrow Q - 2$ in (18) without affecting the gluing conditions. With this we recover the form of the conformal spectrum as derived by Fujimoto and Kawakami³⁴ from the exact solution.^{35,36} By mapping the nontrivial Z_2 part of the two-channel Kondo scattering onto that of a restricted solid-on-solid model³⁷ coupled to the impurity, these authors elegantly circumvented the “string solution” problem mentioned above.

In exact analogy with the single-channel case detailed above, we can match the finite-size two-channel Kondo spectrum defined by Eqs. (18) and (19) to that for the $n_c \rightarrow 1$ limit of the two-channel Anderson model by performing a shift $Q \rightarrow Q - 1$ in Eqs. (18) and (19). The gluing conditions are accordingly modified and now take the form

$$\begin{aligned} Q = 0 \bmod 2, \quad j_s = 0, \text{ or } 1 \quad j_f = \frac{1}{2}, \\ Q = 1 \bmod 2, \quad j_s = \frac{1}{2}, \quad j_f = 0 \text{ or } 1. \end{aligned} \quad (20)$$

The gluing conditions (20) can formally be obtained by starting with the gluing conditions for free electrons (carrying spin and flavor):

$$\begin{aligned} Q = 0 \bmod 2, \quad j_s = 0, \quad j_f = 0, \\ \quad \quad \quad j_s = 1, \quad j_f = 1, \\ Q = 1 \bmod 2, \quad j_s = \frac{1}{2}, \quad j_f = \frac{1}{2}, \end{aligned} \quad (21)$$

and then performing *Kac-Moody fusion with the $j_f = 1/2$ flavor conformal tower*: $j_f = 0 \rightarrow 1/2$; $j_f = 1/2 \rightarrow 0, 1$; $j_f = 1 \rightarrow 1/2$. Alternatively, we can obtain Eqs. (20) from Eqs. (21) by *fusion with the $j_s = 1/2$ spin conformal tower*: $j_s = 0 \rightarrow 1/2$; $j_s = 1/2 \rightarrow 0, 1$; $j_s = 1 \rightarrow 1/2$, *concurrent with fusion with the $Q = 1$ charge conformal tower*: $Q \rightarrow Q + 1$. In Sec. (III.B) we shall see how these two equivalent schemes can be given a simple physical interpretation, considering the particular structure of the hybridization interaction in (4). It is important to realize that in contrast to the single-channel case, the two-channel Kondo gluing conditions in (19) cannot be traded for a local scattering potential by the charge shift $Q \rightarrow Q - 1$. Although a local scattering potential *is* generated [cf. Eq. (23) below] the “charge-renormalized” gluing conditions (20) are *not* those of free electrons. A two-channel Kondo system forms a *non-Fermi liquid* with properties very different from those of phase-shifted free electrons.

Let us now turn to the case of noninteger impurity valence $n_c \neq 1$. As supplementary input we use the fact that the low-lying excited states of the model split into separate gapless charge, spin and flavor excitations for any value of ε (and hence n_c), as revealed by the exact Bethe Ansatz solution.¹⁷ Since there is no change of symmetry of the model as we tune ε_q and ε_s away from the (magnetic two-channel Kondo) limit $\varepsilon \ll \mu - \Gamma$, one expects that a spectral U(1) charge, SU(2)₂ spin, and SU(2)₂ flavor Kac-Moody structure is retained throughout the full range of magnetic and quadrupolar energies. This implies that in the absence of any relevant operators (that could push the model to a fixed point of a different Kac-Moody structure), the finite-size spectrum must take the form

$$E = E_0 + \frac{\pi}{\ell} \left[\left(\frac{1}{8} (Q - n_c)^2 - \frac{1}{8} n_c^2 + N_c \right) + \left(\frac{j_s(j_s + 1)}{4} + N_s \right) + \left(\frac{j_f(j_f + 1)}{4} + N_f \right) \right] \quad (22)$$

with the values of the charge- spin- and flavor- quantum numbers constrained by Eqs. (20). Note that the charge levels have again been shifted by a constant so that Q measures the number of conduction electrons added to or removed from the groundstate [i.e. $E_0 = E(Q = 0)$].

Similar to the ordinary Anderson model, the charge spectrum in (22) implies the presence of an *effective* local scattering potential

$$V_{eff} = -\frac{n_c}{4}J(0). \quad (23)$$

The charge current J has scaling dimension $\Delta = 1$, making V_{eff} in Eq. (23) into an exactly marginal boundary operator with the scaling field sampling the impurity charge valence n_c . Provided that no relevant operators intervene under renormalization, it produces a line of stable fixed points parameterized by the value of n_c or, equivalently, ε . This is in accordance with the Bethe Ansatz solution,¹⁷ which established a line of low-temperature fixed points analytically connected to the overscreened two-channel (magnetic) Kondo fixed point at $\varepsilon \ll \mu - \Gamma$.

Given the finite-size spectrum defined by Eqs. (20) and (22) we shall next identify the leading operator content of the scaling theory, following the “double-fusion” prescription outlined in Sec. II. In particular, we must check that no relevant operators are generated as we vary ε and move away from the integer valence limit $n_c = 1$.

Performing a second Kac-Moody fusion²⁰ with the $j_f = 1/2$ flavor conformal tower, the gluing conditions (20) change to

$$\begin{aligned} Q &= 0 \pmod{2}, & j_s &= 0 \text{ or } 1, & j_f &= 0 \text{ or } 1, \\ Q &= 1 \pmod{2}, & j_s &= \frac{1}{2}, & j_f &= \frac{1}{2}. \end{aligned} \quad (24)$$

These new gluing conditions ensure that the boundary condition in the half-plane geometry is time independent (corresponding to having attached an Anderson impurity to each edge, $x = 0$ and $x = \ell$, of the strip; cf. Sec. II). As we are now effectively considering a finite-size spectrum with *two* quantum impurities present, the charge quantum number gets renormalized twice, with $Q \rightarrow Q - n_c(x = 0) \equiv Q'$ from the impurity at the $x = 0$ edge, and $Q' \rightarrow Q' - n_c(x = \ell) = Q' + n_c(x = 0) = Q$ from the $x = \ell$ edge. Thus, the modifications of Q caused by n_c at each edge of the strip cancel each other, and the double-fusion spectrum becomes independent of the impurity valence. The reason for the cancellation is the same as in the single-channel case, where the sum rule (15) connects n_c to the scattering phase shift caused by the impurity. Since the phase shifts at $x = 0$ and $x = \ell$ have opposite signs (at one edge a left-moving electron is reflected, while at the other edge a right-moving electron gets reflected), one must formally assign charge valences of opposite signs to the auxiliary impurities attached to $x = 0$ and $x = \ell$, respectively. We clearly expect the same situation to apply also in the two-channel case. By comparison with Eqs. (8) and (18) we thus read off for the

possible boundary scaling dimensions $\Delta = \Delta_c + \Delta_s + \Delta_f$:

$$\begin{aligned} \Delta_c &= \frac{1}{8}Q^2 + N_c, \\ \Delta_s &= \frac{1}{4}j_s(j_s + 1) + N_s, & \Delta_f &= \frac{1}{4}j_f(j_f + 1) + N_f \end{aligned} \quad (25)$$

with Q , j_s , and j_f constrained by (24), and with N_c, N_s, N_f positive integers.

The gluing conditions in Eqs. (24) are identical to those for the spectrum of boundary scaling dimensions in the two-channel Kondo model.¹⁹ Here we obtained them by double fusion with the $j_f = 1/2$ flavor conformal tower, while in the Kondo case they follow from double fusion with the spin-1/2 conformal tower. The equivalence of the two procedures is consistent with the $Q \pmod{2}$ invariance of Eqs. (24). Double fusion with $j_f = 1/2$ in the empty valence limit turns into double fusion with $j_s = 1/2$ in the Kondo limit with a concurrent charge renormalization $Q \rightarrow Q + 2$. We shall elaborate on this point in the next section.

The symmetries of the Hamiltonian in Eq. (1) impose further restrictions on the allowed Kac-Moody charge, spin and flavor quantum numbers. Charge conservation implies that $Q = 0$ in Eq. (25) and hence only the trivial identity conformal tower in the charge sector contributes to the spectrum of boundary scaling dimensions. Moreover, since the charge valence n_c does not appear in Eqs. (25), no scaling dimension can depend on it. No relevant operator can therefore appear as n_c is tuned away from the magnetic two-channel Kondo limit. This guarantees that the finite-size spectrum defined by Eqs. (24) and (25) remains valid throughout the full range of charge valence $n_c \in (0, 1)$, with a line of stable fixed points parametrized by n_c . Recall that this line is produced by the marginal operator V_{eff} in Eq. (23), associated with the “single-fusion” spectrum, Eqs. (20) and (22), which carries an explicit dependence on n_c . V_{eff} here plays the role of a *boundary changing* operator.⁴⁴ For a given value of n_c it determines the locus on the fixed line to which the theory flows under renormalization. It may be tempting to conclude that the result obtained from double fusion, Eqs. (24) and (25), implies that the time-independent critical behavior is the *same* along the critical line, being insensitive to n_c . This is correct with regard to *critical exponents*, but as we shall see below, *amplitudes* of various scaling operators pick up a dependence on n_c , giving rise to very different physics as we move along the fixed line.

The leading boundary operator contributed by the charge sector is the exactly marginal charge current $J(0) =: \psi_{\alpha\sigma}^\dagger(0)\psi_{\alpha\sigma}(0) :$. It is formally identified as the first Kac-Moody descendant²⁵ $J(0) = J_{-1}\mathbb{1}^{(c)}(0)$ of the identity operator $\mathbb{1}^{(c)}$ (which generates the $Q = 0$ conformal tower). As we have seen, $J(0)$ being marginal, it shows up manifestly in the low-energy spectral-generating Hamiltonian H_{charge} in Eq. (17), and is responsible for producing the line of fixed points.

The appearance of the charge current breaks particle-hole symmetry, since $J(0) \rightarrow -J(0)$ under charge conjugation $\psi_{\alpha\sigma}(x) \rightarrow \epsilon_{\alpha\beta}\epsilon_{\sigma\mu}\psi_{\beta\mu}^\dagger(x)$. It is interesting to note that while the same symmetry is broken by the ionic pseudoparticle term (3) in (1) under $f_\sigma^\dagger \rightarrow \epsilon_{\sigma\mu}f_\mu$, the pieces (2) and (4) of the Hamiltonian involving the conduction electron field $\psi_{\alpha\sigma}(x)$ actually respect charge conjugation. This symmetry gets broken dynamically via the coupling to the pseudo-particles, allowing the charge current in Eq. (23) to enter the stage.³⁸

The next-leading boundary operator from the charge sector is that of the energy-momentum tensor, $T^{(c)}(0) = :J(0)J(0):/4$, appearing as the second *Virasoro descendant*²⁵ of the identity operator, $T_c(0) = L_{-2}\mathbb{1}^{(c)}(0)$. Although it carries scaling dimension $\Delta = 2$ and hence is subleading to the charge current $J(0)$, being a Virasoro descendant of the identity operator it has a nonvanishing expectation value and turns out to produce the same scaling in temperature as $J(0)$. Although not central to the present problem, we shall briefly return to this question in Sec. IV.

Focusing now on the spin and flavor sectors, conservation of total spin and flavor quantum numbers requires that all spin and flavor boundary operators must transform as singlets. The leading spin boundary operator with this property, $\mathcal{O}^{(s)}(0)$ call it, has dimension $\Delta_s = 3/2$ and is obtained by contracting the spin-1 field $\phi^{(s)}(0)$ (which generates the $j_s = 1$ conformal tower) with the vector of $SU(2)_2$ raising operators $\mathbf{J}_{-1}^{(s)} : \mathcal{O}^{(s)}(0) = \mathbf{J}_{-1}^{(s)} \cdot \phi^{(s)}(0)$. As expected, this is the same operator that drives the critical behavior in the two-channel (magnetic) Kondo problem.¹⁹ The next-leading spin boundary operator is the energy momentum tensor $T^{(s)}(0) = : \mathbf{J}^{(s)}(0) \cdot \mathbf{J}^{(s)}(0) : /4 [= L_{-2}\mathbb{1}^{(s)}(0)]$, of dimension $\Delta_s = 2$.

The two leading flavor boundary operators are obtained in exact analogy with the spin case. In obvious notation: $\mathcal{O}^{(f)}(0) = \mathbf{J}_{-1}^{(f)} \cdot \phi^{(f)}(0)$ of dimension $\Delta_f = 3/2$, and $T^{(f)}(0) = : \mathbf{J}^{(f)}(0) \cdot \mathbf{J}^{(f)}(0) : [= L_{-2}\mathbb{1}^{(f)}(0)]$ of dimension $\Delta_f = 2$.

Boundary operators with integer scaling dimensions generate an analytic temperature dependence of the impurity thermodynamics,²⁰ subleading to that coming from the two leading irrelevant operators $\mathcal{O}^{(s)}(0)$ and $\mathcal{O}^{(f)}(0)$. Hence, in what follows we shall focus on these latter operators. In the case of the two-channel Kondo problem the flavor operator $\mathcal{O}^{(f)}(0)$ was argued to be effectively suppressed, at least for the case when the (bare) Kondo coupling is sufficiently small.¹⁹ On dimensional grounds one expects that the spin scaling field λ_s [multiplying $\mathcal{O}^{(s)}(0)$ in the scaling Hamiltonian] is $O(1/\sqrt{T_K})$, where T_K is the Kondo scale for the crossover from weak coupling (high-temperature phase) to strong renormalized coupling (low-temperature phase). The flavor operator, on the other hand, does not see this scale since the infrared divergences in perturbation theory (which signal the appearance of a dynamically generated scale) occur

only in the spin sector. The only remaining scale is that of the band width D (which plays the role of an ultraviolet cutoff), implying that the flavor scaling field λ_f [multiplying $\mathcal{O}^{(f)}(0)$] is $O(1/\sqrt{D})$. For a small (bare) Kondo coupling λ , $T_K \sim D \exp(-1/\lambda) \ll D$, and the critical behavior is effectively determined by $\mathcal{O}^{(s)}(0)$ alone.

As we will show, the picture changes dramatically for the two-channel Anderson model. The Bethe Ansatz solution¹⁷ shows that there are *two* dynamically generated temperature scales $T_\pm(\varepsilon)$ present in this model. They determine and parametrize the thermodynamic response of the system. Consider for example the quenching of the entropy as the temperature is lowered: in the magnetic moment regime ($\varepsilon \ll \mu - \Gamma$) the two scales are widely separated, $T_+ \ll T_-$. For temperatures in the range $T_+ \leq T \leq T_-$ charge and flavor fluctuations are suppressed and the entropy shows a plateau corresponding to the formation of a local moment. The moment undergoes frustrated screening when the temperature is lowered below T_- reaching zero point entropy $S = k_B \ln \sqrt{2}$, and $n_c = 1$. As ε decreases T_+ and T_- approach each other and the range over which the magnetic moment exists decreases too. It disappears (i.e. $T_+ = T_-$) when $\varepsilon = \mu$. At this point no magnetic moment forms. However the system still flows to a frustrated two-channel Kondo fixed point, with entropy $S = k_B \ln \sqrt{2}$, but with $n_c = 1/2$. Continuing along the critical line, the two scales trade places, and eventually, at the quadrupolar critical endpoint ($\varepsilon \gg \mu - \Gamma$), one finds that $T_+ \gg T_-$. Since the irrelevant spin (flavor) operator is expected to dominate the critical behavior at the magnetic (quadrupolar) fixed point, we are led to conjecture that the corresponding scaling field is parametrized precisely by $1/\sqrt{T_+}$ ($1/\sqrt{T_-}$). With this scenario played out, the relative importance of the two boundary operators changes continuously as one moves along the fixed line, with each operator ruling at its respective critical endpoint.

In the next section we shall prove our conjecture by computing the impurity specific heat and susceptibility following from the scaling Hamiltonian and comparing it to the low temperature thermodynamics from the exact Bethe Ansatz solution.¹⁷ We shall also use this comparison to “fit” the parametrization of the scaling fields. This fixes the critical theory completely.

B. Application: Fermi Edge Singularities

Before taking on this task, however, we shall exploit the BCFT scheme developed above to determine the scaling dimensions of the pseudoparticles which enter the Hamiltonian in (3) and (4). The analogous problem for the ordinary Anderson model has been extensively studied^{39,40,41}, in part because of its close connection to the *X-ray absorption problem*.

One is here interested in the situation where X-ray absorption knocks an electron from a filled inner shell

of an ion in a metal into the conduction band. As an effect the conduction electrons experience a transient local potential at the ion which lost the core electron, and this typically produces a singularity in the X-ray spectrum $\sim (\omega - \omega_F)^{-\beta}$ close to the Fermi level threshold ω_F . Nozieres and de Dominicis,⁴² using a simple model, showed that the exponent β depends only on the phase shift which describes the scattering of conduction electrons from the core hole created by the X-ray. Fermi edge singularities linked to local dynamic perturbations are fairly generic,⁴³ and it is therefore interesting to explore how they may appear in a slightly more complex situation where a localized “deep hole” type perturbation involves additional degrees of freedom. Indeed, the two-channel Anderson model in Eq. (1) provides an ideal setting for this as it accommodates a local quantum impurity carrying both spin *and* channel (quadrupolar) degrees of freedom.

To set the stage, let us make a *Gedankenexperiment* and imagine that we suddenly replace a thorium ion in the host metal (say, $U_{0.9}Th_{0.1}Be_{13}$) by a uranium ion, the sole effect being to introduce a localized quadrupolar *or* magnetic moment. To describe the response of the host to this perturbation, we consider the pseudoparticle propagators

$$G_\sigma = \langle 0 | e^{iHt} f_\sigma e^{-iHt} f_\sigma^\dagger | 0 \rangle \quad (26)$$

$$G_{\bar{\alpha}} = \langle 0 | e^{iHt} b_{\bar{\alpha}} e^{-iHt} b_{\bar{\alpha}}^\dagger | 0 \rangle \quad (27)$$

(with no summation over α, σ). At time $t < 0$ the ground state $|0\rangle$ of the metal is that of free conduction electrons. At $t = 0$ a pseudoparticle (creating the localized moment) is inserted into the metal, and the system evolves

in time governed by the two-channel Anderson Hamiltonian in Eq. (1). At some later time t the pseudo-particle is removed, and one measures the overlap between the state obtained with the initial unperturbed groundstate. It is important to realize that by inserting (removing) a pseudoparticle operator, one simultaneously turns on (off) the impurity terms in Eqs. (3) and (4), and hence changes the dynamics of the conduction electrons. As we reviewed in Sec. (II), at low temperatures and close to a critical point, this corresponds to a change of the boundary condition which emulates the presence (absence) of the impurity. Hence, the pseudoparticle operators f_σ and b_α are *boundary changing operators*,²⁶ and we can use the BCFT machinery to calculate their propagators in Eqs. (26) and (27). Our discussion closely follows that in Ref. 44.

We start by considering the free-electron theory defined on the complex upper half-plane $\mathbb{C}^+ = \{z = \tau + ix; x \geq 0\}$ with a trivial (Fermi liquid) boundary condition, call it “A”, imposed at the real axis $x = 0$. We denote by $|A; 0\rangle$ the ground state for this configuration. By injecting a pseudoparticle at time $\tau = 0$, the boundary condition for $\tau > 0$ changes to “B”, here labeling the boundary condition which corresponds to the nontrivial gluing condition in (20) for the spectrum of the two-channel Anderson model. By mapping the half-plane to a strip $\{w = u + iv; 0 \leq v \leq \ell\}$ via the conformal transformation $w = (\ell/2\pi) \ln z$, the boundary of the strip at $v = \ell$ also turns into type B after insertion of the pseudoparticle operator. Under the same transformation the pseudoparticle propagator in \mathbb{C}^+ , $\langle A; 0 | \mathcal{O}_i(\tau_1) \mathcal{O}_i^\dagger(\tau_2) | A; 0 \rangle = (\tau_1 - \tau_2)^{-2x_i}$ (with x_i the dimension of \mathcal{O}_i , $i = f$ or b) transforms as

$$(\tau_1 - \tau_2)^{-2x_i} \rightarrow \left(\frac{2\ell}{\pi} \sinh \frac{\pi}{2\ell} (u_1 - u_2) \right)^{-2x_i} = \sum_n | \langle AA; 0 | \mathcal{O}_i(0) | AB; n \rangle |^2 e^{-(E_n^{AB} - E_0^{AA})(u_2 - u_1)}, \quad (28)$$

where on the right-hand side of Eq. (28) we have inserted a complete set of states $|AB; n\rangle$, $n = 0, 1, \dots$ of energies E_n^{AB} , defined on the strip with boundary condition A (B) at $u = 0$ ($u = \ell$). In the limit $u_2 - u_1 \gg \ell$:

$$\left(\frac{2\ell}{\pi} \sinh \frac{\pi}{2\ell} (u_1 - u_2) \right)^{-2x_i} \rightarrow \frac{\pi}{\ell} e^{-[\pi x_i (u_2 - u_1) / \ell]}. \quad (29)$$

It follows, by comparison with Eq. (28), that

$$x_i = \frac{\ell}{\pi} (E_{n_i}^{AB} - E_0^{AA}), \quad (30)$$

where n_i is the lowest energy state with a nonzero matrix element in the sum in Eq. (28).

The pseudoparticle spectrum $I_i(\omega)$ close to the Fermi level is obtained by Fourier transforming the corresponding propagator in Eq. (26) or (27), and it follows that

$$I_i(\omega) \sim \frac{1}{|\omega - \omega_F|^{1-2x_i}}, \quad i = f, b, \quad (31)$$

with a singularity when $x_i < 1/2$.

Let us consider first the slave boson b_α , carrying quantum numbers $Q = 0, j_s = 0, j_f = 1/2$. Its scaling dimension x_b is given by Eq. (30) where $E_{n_i}^{AB}$ is obtained from Eq. (22) by putting $Q = 0, j_s = 0, j_f = 1/2$, and with $E_0^{AA} = 0$ (with proper normalization of energies). To be able to compare energies corresponding to different boundary conditions it is important to keep the overall energy normalization fixed, and hence we must remove the normalization constant $-\pi n_c^2 / 8\ell$ in Eq. (22) before reading off the answer. (Recall that this normalization constant is expressly designed to remove the $Q = 0$ con-

tribution from the charge sector to the ground state energy.) We thus obtain

$$x_b = \frac{3}{16} + \frac{1}{8}n_c^2. \quad (32)$$

Similarly, we obtain for the pseudo fermion ($Q = 1, j_s = 1/2, j_f = 0$):

$$x_f = \frac{5}{16} - \frac{1}{4}n_c + \frac{1}{8}n_c^2. \quad (33)$$

It is interesting to compare Eqs. (32) and (33) with the corresponding scaling dimensions in the ordinary Anderson model, obtained in Refs. 39,41: $x'_b = n_c^2/2, x'_f = 1/2 - n_c/2 + n_c^2/4$. We conclude that by opening an additional channel for the electrons, the singularity in the slave boson spectrum in Eq. (31) (corresponding to X-ray photoemission) gets softer, whereas for the pseudofermion spectrum (corresponding to X-ray absorption) the opposite is true. One can show that this trend is systematic, and gets more pronounced as the number of channels increases.⁴⁵ We also note that the values of the pseudoparticle scaling dimensions as obtained by various approximation schemes, e.g. the "non-crossing approximation" (NCA) and large- N calculations,⁴⁶ are not in agreement with the exact results presented here.

Before closing this section, let us return to the *Gedankenexperiment* where we inserted an empty (degenerate) impurity level by adding a slave boson to the filled Fermi sea. The slave boson carries only flavor $j_f = 1/2$, and it follows that the allowed values of the quantum numbers of the combined system are obtained by coupling $j_f = 1/2$ to the flavor quantum numbers j'_f of the conduction electrons (leaving charge and spin untouched). Since j_f and j'_f label conformal towers, this coupling is *precisely governed by conformal fusion with $j_f = 1/2$* : $j'_f \rightarrow |j'_f - 1/2|, |j'_f - 1/2| + 1, \dots, \min(j'_f + 1/2, 3/2 - j'_f)$. By letting the system relax, a non-zero charge valence n_c may then build up at the impurity site (as determined by the particular value of $\varepsilon = \varepsilon_s - \varepsilon_q$). Formally, this process is captured by the charge renormalization $Q \rightarrow Q - n_c$ in the finite size-spectrum (22), taking place concurrently with the fusion in flavor space which produces the nontrivial gluing conditions (20). Running the *Gedankenexperiment* with a pseudo-fermion instead (carrying charge and spin, but no flavor) leads to a scenario dual to the one above, where the coupling is now governed by fusion with $j_s = 1/2$ in the spin sector and $Q = 1$ in the charge sector [cf. the discussion after Eq. (21)]. As the system relaxes an average charge n_c goes to the impurity site, again leading to the renormalization $Q \rightarrow Q - n_c$ in the spectrum (22). We conclude that our key results, Eqs. (20) and (22) – obtained in Sec (II.A) via a formal analysis – can be given a natural interpretation by considering the pseudoparticle structure of the hybridization interaction in Eq. (4).

IV. LOW-TEMPERATURE THERMODYNAMICS

A. Zero-Temperature Entropy

The Bethe Ansatz solution¹⁷ of the model reveals that the line of fixed points is characterized by a zero-temperature entropy $S_{imp} = k_B \ln \sqrt{2}$ typical of the two-channel Kondo fixed point. As we shall show next, this property emerges naturally when feeding in our result from Sec. (II.A) into the general BCFT formalism developed by Cardy.²⁶

Recall that the key ingredient in this formalism is the *modular invariance*²⁴ of a conformal theory. Applied to a model defined on a cylinder of circumference $\beta = 1/T$ and length ℓ , and with conformally invariant boundary conditions A and B imposed at the open ends, this means that its partition function Z_{AB} is invariant under exchange of space and (Euclidean) time variables. In our case, B is the boundary condition obtained from A by attaching an Anderson impurity to one of the edges of the cylinder (with A a trivial Fermi liquid boundary condition, to be defined below). Now, let H^* be the critical Hamiltonian that corresponds to the spectrum given by Eqs. (20) and (22). Then $H_{AB} \equiv (\ell/\pi)H^*$ generates time translations around the cylinder specified above. The partition function Z_{AB} can hence be written

$$Z_{AB} = \text{Tr} e^{-\beta H_{AB}} = \sum_a n_{AB}^a \chi_a(e^{-\pi\beta/\ell}). \quad (34)$$

Here χ_a is a character of the conformal $U(1) \times SU(2)_2 \times SU(2)_2$ algebra, with $a = (Q, j_s, j_f)$ labeling a product of charge, spin, and flavor conformal towers [constrained by Eqs. (21)], and with n_{AB}^a counting its degeneracy within the spectrum of H_{AB} . By a modular transformation $\beta \leftrightarrow \ell$ the role of space and time is exchanged, and the partition function now gets expressed as

$$Z_{AB} = \langle A | e^{-\ell H_\beta} | B \rangle, \quad (35)$$

where H_β is the transformed Hamiltonian generating translations *along* the cylinder, in the space direction, with $|A\rangle$ and $|B\rangle$ *boundary states*²⁶ implicitly defined by Eq. (35). By inserting a complete set of *Ishibashi states* $|a\rangle = \sum_m |a; m\rangle_L \otimes |a; m\rangle_R$ into Eq. (35) (with m running over all states in an L/R product of charge, spin, and flavor conformal towers labelled by the index a , one obtains²⁴

$$Z_{AB} = \sum_a \langle A | a \rangle \langle a | B \rangle \chi_a(e^{-4\pi\ell/\beta}). \quad (36)$$

Equating Eqs. (34) and (36) one can immediately read off *Cardy's equation*²⁶

$$\sum_b n_{AB}^b S_{ab} = \langle A | a \rangle \langle a | B \rangle, \quad (37)$$

where S_{ab} is the *modular S matrix* defined by

$$\chi_a(e^{-\pi\beta/\ell}) = \sum_b S_{ab} \chi_b(e^{-4\pi\ell/\beta}), \quad (38)$$

with a and b indexing products of charge, spin, and flavor conformal towers. It follows that the nontrivial boundary state $|B\rangle$ (which emulates the presence of the impurity) is related to $|A\rangle$ via the identity²⁶

$$\langle a|B\rangle = \langle a|A\rangle \frac{S_{ad}}{S_{a0}}, \quad (39)$$

with 0 labeling the product of identity conformal towers and d the product of conformal towers with which the Kac-Moody fusion of the finite-size spectrum is performed. As we found in Sec. (II.A), for the two-channel Anderson model, $d = (Q=0, j_s=0, j_f=1/2)$. Factoring the modular S matrices in charge, spin, and flavor, with $a = (Q, j_s, j_f)$ constrained by Eqs. (21) but otherwise arbitrary, one obtains

$$\frac{S_{ad}}{S_{a0}} = \frac{S_{Q0}^c S_{j_s0}^s S_{j_f1/2}^f}{S_{Q0}^c S_{j_s0}^s S_{j_f0}^f} = \frac{S_{j_f1/2}^f}{S_{j_f0}^f}. \quad (40)$$

The modular S matrix for the $SU(2)_2$ flavor symmetry is given by²⁴

$$S_{j_f j'_f} = \frac{1}{\sqrt{2}} \sin \left[\frac{\pi(2j_f + 1)(2j'_f + 1)}{4} \right], \quad (41)$$

and it follows from Eqs. (39) and (40) that

$$\langle a|B\rangle = \langle a|A\rangle \frac{\sin[\frac{\pi}{2}(2j_f + 1)]}{\sin[\frac{\pi}{4}(2j_f + 1)]}. \quad (42)$$

We now have the tools for deriving the impurity entropy. Following the analogous analysis of the multichannel Kondo model in Ref. 47 we take the limit $\ell/\beta \rightarrow \infty$ in Eq. (36) (i.e. we take $\beta \rightarrow \infty$ *after* the large-volume limit $\ell \rightarrow \infty$). As a result, only the character of the ground-state, $\chi_{a=(0,0,0)}(e^{-4\pi\ell/\beta}) = e^{\pi\ell c/6\beta}$, contributes to Z_{AB} (with c the conformal anomaly of the theory). One thus obtains

$$Z_{AB} \rightarrow e^{\pi\ell c/6\beta} \langle A|0\rangle \langle 0|B\rangle, \quad \ell/\beta \rightarrow \infty, \quad (43)$$

with $|0\rangle \equiv |Q=0, j_s=0, j_f=0\rangle$. The free energy is thus

$$F_{AB} = -\pi c k_B T^2 \ell/6 - k_B T \ln(\langle A|0\rangle \langle 0|B\rangle). \quad (44)$$

The second term in Eq. (44) is independent of the size ℓ of the system, and we therefore identify

$$S_{imp} = k_B \ln(\langle A|0\rangle \langle 0|B\rangle) \quad (45)$$

as the impurity contribution to the zero-temperature entropy. With no impurity present, $A=B$ and $S_{imp}=0$, and it follows that $|A\rangle = |0\rangle$ [consistent with the *Fermi liquid gluing condition* in Eq. (21)]. Thus, from Eqs. (42) and (45) we finally get

$$S_{imp} = k_B \ln \sqrt{2}, \quad (46)$$

in agreement with the Bethe Ansatz result in Ref. 17.

A few remarks may here be appropriate. First, we note that the effective renormalization of the charge sector, $Q \rightarrow Q - n_c$ [cf. Eq. (22)], does *not* influence the impurity entropy. At first glance, this may seem obvious: the degeneracies of the impurity levels – and hence the impurity entropy – is *a priori* not expected to be affected by the potential scattering in (23) caused by the impurity valence n_c . The picture becomes less trivial when one realizes that the impurity valence in fact controls *how* the spin and flavor degrees of freedom get screened by the electrons. As found in the Bethe Ansatz solution¹⁷, for nonzero $\varepsilon = \varepsilon_s - \varepsilon_q$, the quenching of the entropy occurs in two stages as the temperature is lowered. For sufficiently large values of $|\varepsilon - \mu|$, the free impurity entropy $k_B \ln 4$ is first reduced to $k_B \ln 2$ at an intermediate temperature scale, suggestive of a single remnant magnetic *or* quadrupolar moment (depending on the sign of ε or, equivalently, the sign of $n_c - 1/2$). As the temperature is lowered further, this moment gets overscreened by the conduction electrons, as signaled by the residual entropy $k_B \ln \sqrt{2}$. Remarkably, as found in Ref. 17 and verified here within the BCFT formalism, the *same* residual impurity entropy $k_B \ln \sqrt{2}$ appears also in the mixed-valence regime $|\varepsilon - \mu| \leq \Gamma$ (where $n_c \approx 1/2$), for which there is no single localized moment present at any temperature scale.

B. Impurity Specific Heat

We now turn to the calculation of the impurity specific heat. Again, the analysis closely parallels that for the two-channel Kondo model.¹⁹ Some elements are new, however, and we here try to provide a self-contained treatment.

First, we need to write down the scaling Hamiltonian $H_{scaling}$ that governs the critical behavior close to the line of boundary fixed points. To leading order it is obtained by adding the dominant boundary operators found in Sec (III) to the bulk critical Hamiltonian H^* [representing H_{bulk} in Eq. (1)]:

$$H_{scaling} = H^* + \lambda_c J(0) + \lambda_s \mathcal{O}^{(s)}(0) + \lambda_f \mathcal{O}^{(f)}(0) + \text{subleading terms}, \quad (47)$$

with $\lambda_{c,s,f}$ the corresponding conjugate scaling fields. As reflected in the finite-size spectrum (22), H^* splinters into dynamically independent charge, spin, and flavor pieces, implying, in particular, that all correlation functions decompose into products of independent charge, spin and flavor factors. *On* the critical line the impurity terms H_{ion} and H_{hybr} in Eqs. (3) and (4) together masquerade as a boundary condition on H^* , coded in the nontrivial gluing conditions in Eqs. (20). In addition H_{ion} and H_{hybr} also give rise to the exactly marginal charge current term $\lambda_c J(0)$ in Eq. (47). This term keeps track of the charge valence acquired by the impurity. As

we have already noticed, this is different from the Kondo problem where the local spin exchange interaction at criticality gets *completely* disguised as a conformal boundary condition.²⁰ The reason for the difference is that away from the (integer valence) Kondo limit, the effective local scattering potential in Eq. (23) cannot be removed by redefining the charge quantum numbers $Q \rightarrow Q - 2$ in Eqs. (20) and (22). This in turn reflects the fact that for non-integer valence the dynamics manifestly breaks particle-hole symmetry, whereas for integer valence there is an equivalent description¹⁷ in terms of the two-channel Kondo model where this symmetry is restored³⁸. *Off* the critical line the impurity terms in Eqs. (3) and (4) appear in the guise of irrelevant boundary terms, of which

$\lambda_s \mathcal{O}^{(s)}(0)$ and $\lambda_f \mathcal{O}^{(f)}(0)$ in Eq. (47) are the leading ones.

Recall from Sec. (II) that a boundary critical theory by default is defined in the complex half-plane $\mathbb{C}^+ = \{\text{Im } z > 0\}$, with the boundary condition imposed on the real axis $\text{Im } z = 0$. As we have seen, by continuing the fields to the lower half-plane we obtain a *chiral* representation of this theory, now defined in the full complex plane \mathbb{C} . Via the transformation $w = \tau + ix = (\beta/\pi) \arctan(z)$, \mathbb{C} can be mapped conformally onto an infinite cylinder, Γ_c call it, of circumference β : $\Gamma_c = \{(\tau, x); -\beta/2 \leq \tau \leq \beta/2; -\infty \leq x \leq \infty\}$. It is convenient to use Γ_c as a “finite-temperature geometry” by treating β as an inverse temperature. The partition function can then be written as

$$e^{-\beta F(\beta, \{\lambda_\nu\})} = e^{-\beta F(\beta, 0)} \langle \exp \left(\int_{-\beta/2}^{\beta/2} d\tau [\lambda_c \tilde{J}(\tau, 0) + \lambda_s \tilde{\mathcal{O}}^{(s)}(\tau, 0) + \lambda_f \tilde{\mathcal{O}}^{(f)}(\tau, 0)] + \text{subleading terms} \right) \rangle_T, \quad (48)$$

where $F(\beta, \{\lambda_\nu\}) = F_{\text{bulk}}(\beta, 0) + f_{\text{imp}}(\beta, \{\lambda_\nu\})$ is the sum of bulk and impurity free energies, with $\{\lambda_\nu\} \equiv (\lambda_c, \lambda_s, \lambda_f, \dots)$ the collection of boundary scaling fields. We have here passed to a Lagrangian formalism, with the “tilde” and $\langle \rangle_T$ referring to the finite- T geometry Γ_c . By a linked cluster expansion we obtain from Eq. (48) the impurity contribution to the free energy:

$$f_{\text{imp}}(\beta, \{\lambda_\nu\}) = -\frac{1}{2\beta} \iint_{-\beta/2}^{\beta/2} d\tau_1 d\tau_2 [\lambda_c^2 \langle \tilde{J}(\tau_1, 0) \tilde{J}(\tau_2, 0) \rangle_{T,c} + \sum_{\nu=s,f} \lambda_\nu^2 \langle \tilde{\mathcal{O}}^\nu(\tau_1, 0) \tilde{\mathcal{O}}^\nu(\tau_2, 0) \rangle_{T,c}] + \text{subleading terms}, \quad (49)$$

with $\langle \rangle_{T,c}$ denoting a connected two-point function in Γ_c and where, for a fixed temperature $1/\beta$, the constant term $f_{\text{imp}}(\beta, 0)$ has been subtracted. Note that the linear terms in the expansion are absent since all three boundary operators are Virasoro primary²⁴ and hence have vanishing expectation values. Since two-point functions containing operators from different sectors (charge, spin or flavor) decompose into products of one-point functions, these also vanish. Similarly, connected two-point functions reduce to ordinary two-point functions. Also note that there is no term in Eq. (49) of zeroth order in the scaling fields. This is a generic feature of quantum impurity problems, which is best understood by looking at the finite-size scaling form⁴⁸ for the impurity free energy:

$$f_{\text{imp}}(\beta, \{\lambda_\nu\}) = E_{\text{imp}} + \frac{1}{\beta} Y_{\text{imp}}(\{\lambda_\nu \beta^{y_\nu}\}) + \dots, \quad (50)$$

with Y_{imp} a universal scaling function and E_{imp} nonuniversal. The exponents y_ν are RG eigenvalues, connected to the dimensions Δ_ν of the irrelevant boundary operators by $y_\nu = 1 - \Delta_\nu$. It follows immediately from Eq. (50) that *at* the fixed point

$$C_{\text{imp}}(\{\lambda_\nu = 0\}) = -T \frac{\partial^2 f_{\text{imp}}}{\partial T^2} = 0. \quad (51)$$

Thus, to see the effect of the impurity, the leading irrelevant boundary operators have to be added explicitly, and these operators then produce the dominant terms in the scaling in temperature.

The correlation function of chiral Virasoro primary operators $\mathcal{O}^{(i)}$ in \mathbb{C} takes the familiar form

$$\langle \mathcal{O}^{(i)}(z_1) \mathcal{O}^{(i)}(z_2) \rangle = \frac{A_i}{(z_1 - z_2)^{2\Delta_i}}. \quad (52)$$

Here Δ_i is the scaling dimension of $\mathcal{O}^{(i)}$, and A_i is a normalization constant. Mapping the real axis $\text{Im } z = 0$ into Γ_c , this transforms into

$$\langle \tilde{\mathcal{O}}^{(i)}(\tau_1, 0) \tilde{\mathcal{O}}^{(i)}(\tau_2, 0) \rangle_T = \frac{A_i}{\left| \frac{\beta}{\pi} \sin\left(\frac{\pi}{\beta}(\tau_1 - \tau_2)\right) \right|^{2\Delta_i}}, \quad (53)$$

and it follows that Eq. (49) can be rewritten as

$$f_{imp}(\beta, \{\lambda_\nu\}) = -\frac{1}{2\beta} \int_{\tan\kappa}^{\infty} du \left(\lambda_c^2 A_c \frac{1}{u^2} + (\lambda_s^2 A_s + \lambda_f^2 A_f) \frac{\sqrt{1+u^2}}{u^3} \right) + \text{subleading terms}, \quad (54)$$

with κ a UV cutoff. This form is obtained by replacing the double integral in Eq. (49) by a single integral over $\tau = \tau_1 - \tau_2$, exploiting that the two-point functions in Eq. (53) are periodic in τ (with period β). Introducing the auxiliary variable $u \equiv \tan(\pi\tau/\beta)$ and specifying the scaling dimensions $\Delta_c = 1, \Delta_s = \Delta_f = 3/2$ in Eq. (53),

one arrives at the expression in Eq. (54) after inserting the short-time cutoff $\tau_0 = \kappa\beta/\pi$. The integral can be evaluated straightforwardly^{19,49} and in the limit of low temperatures, i.e. for small κ , an expansion of $\tan(\kappa)$ yields for the impurity specific heat:

$$C_{imp} = -T \frac{\partial^2 f_{imp}}{\partial T^2} = (\lambda_s^2 A_s + \lambda_f^2 A_f) \pi^2 T \ln\left(\frac{1}{\tau_0 T}\right) + \lambda_c^2 A_c \pi^2 \tau_0 T + \text{corrections from subleading boundary operators}. \quad (55)$$

Before proceeding, let us comment on the correction terms in Eq. (55). The next-leading boundary operators are the energy-momentum tensors $T^{(c,s,f)}$ identified in Sec. (III.A). Passing to the finite- T geometry Γ_c , their contribution to the partition function takes the form

Inserting Eq. (57) into (56) and integrating, it follows that the contribution to the impurity specific heat is

$$e^{-\beta F(\beta,0)} \left\langle \exp\left(\sum_{i=c,s,f} \int_{-\beta/2}^{\beta/2} d\tau \lambda'_i \tilde{T}^{(i)}(\tau,0)\right) \right\rangle_T, \quad \delta C_{imp} = \frac{\pi^2}{3} \left(\lambda'_c + \frac{3\lambda'_s}{2} + \frac{3\lambda'_f}{2}\right) T. \quad (58)$$

with λ'_i conjugate scaling fields. It follows, again by a linked cluster expansion, that they contribute

$$\delta f_{imp} = -\frac{1}{2\beta} \sum_{i=c,s,f} \int_{-\beta/2}^{\beta/2} d\tau \lambda'_i \langle \tilde{T}^{(i)}(\tau,0) \rangle_T + \text{subleading terms} \quad (56)$$

to the impurity free energy. Note that in contrast to the contribution from the leading boundary operators in Eq. (49), δf_{imp} is linear in the scaling fields λ'_i . This reflects the fact that the energy-momentum tensors are Virasoro descendants of the identity operator, with non-vanishing one-point functions²⁴

$$\langle \tilde{T}^{(i)}(\tau,0) \rangle_T = \frac{d_i}{6} \left(\frac{\pi}{\beta}\right)^2, \quad d_c = 1, \quad d_s = d_f = \frac{3}{2}. \quad (57)$$

This is the leading correction in Eq. (55) that is linear in the scaling fields: higher-order Virasoro descendants of the identity operator generate higher powers in temperature. Similarly, higher-order Kac-Moody descendants of the $\phi^{(s)}$ and $\phi^{(f)}$ operators produce subleading corrections to the impurity specific heat that are quadratic in the scaling fields.

Returning to Eq. (55) it is important to notice that the leading logarithmic terms are independent of the cutoff procedure. We can make this explicit by introducing the temperature scales T_s and T_f that characterize the spin and flavor dynamics, and absorb the arbitrary cutoff τ_0 in the subleading terms:

$$C_{imp} = \lambda_s^2 A_s \pi^2 T \ln\left(\frac{T_s}{T}\right) + \lambda_f^2 A_f \pi^2 T \ln\left(\frac{T_f}{T}\right) + \left(\lambda_c^2 A_c \tau_0 + \lambda_s^2 A_s \ln\left(\frac{1}{\tau_0 T_s}\right) + \lambda_f^2 A_f \ln\left(\frac{1}{\tau_0 T_f}\right) \right) \pi^2 T + \text{subleading terms}. \quad (59)$$

It remains to determine the parameters $\lambda_{s,f}, A_{s,f}$ and

$T_{s,f}$ that enter the leading terms in Eq. (59). Start-

ing with the normalization constants of the two-point functions [cf. Eq. (52)], these are defined by²⁴ $A_{s,f} \equiv \langle \mathbf{J}_{-1}^{(s,f)} \cdot \phi^{(s,f)} | \mathbf{J}_{-1}^{(s,f)} \cdot \phi^{(s,f)} \rangle$. Dropping the indices (s, f) , we have that $\langle \mathbf{J}_{-1} \cdot \phi | \mathbf{J}_{-1} \cdot \phi \rangle = \langle \phi^a | J_1^a J_{-1}^b | \phi^b \rangle = \langle \phi^a | [J_1^a, J_{-1}^b] + J_{-1}^b J_1^a | \phi^b \rangle = \langle \phi^a | [J_1^a, J_{-1}^b] | \phi^b \rangle$, where the last identity follows from $|\phi^b\rangle$ being a Kac-Moody primary state. Using the $SU(2)_2$ Kac-Moody algebra $[J_1^a, J_{-1}^b] = i\epsilon^{abc} J_0^c + \delta^{ab}$ (common for spin and flavor sectors), together with the fact that ϕ transforms as a spin-1 object under global $SU(2)$ (generated by \mathbf{J}_0), one straightforwardly arrives at the result $A_{s,f} = 9$.

Turning to the scaling fields $\lambda_{s,f}$, on dimensional grounds these must take the form

$$\lambda_{s,f} = \frac{B_{s,f}}{\sqrt{T_{s,f}}}, \quad (60)$$

with $B_{s,f}$ dimensionless constants. The scaling fields and temperature scales T_s and T_f (which also enter the logarithms explicitly in Eq. (59)) will be extracted from the numerical solution of the Thermodynamic Bethe Ansatz (TBA).¹⁷ But first we need to discuss the effect of applied external fields.

C. Magnetic Susceptibility

In the presence of a magnetic field B , applied in the \hat{z} direction, the term

$$\int_{-\infty}^{\infty} dx J_s^z(x)$$

must be added to the scaling Hamiltonian in Eq. (47). Here $J_s^z = (1/2) : \psi_{\alpha\mu}^\dagger \sigma_{\mu\nu}^z \psi_{\alpha\nu} :$ is the z component of the electron spin current that couples to the field. Passing to the finite- T geometry Γ_c , this adds a term

$$B \int_{-\infty}^{\infty} dx \int_{-\frac{\beta}{2}}^{\frac{\beta}{2}} d\tau \tilde{J}_s^z(\tau, x)$$

to the impurity effective action in Eq. (48). By a linked cluster expansion to $O(B^2)$, the impurity magnetic susceptibility

$$\chi_{imp} = - \frac{\partial^2 f_{imp}}{\partial B^2} \Big|_{B=0} \quad (61)$$

gets expressed as

$$\begin{aligned} \chi_{imp} = & -\frac{1}{\beta} \sum_{i=c,s,f} \lambda_i \int \int_{-\infty}^{\infty} dx_1 dx_2 \int \dots \int_{-\frac{\beta}{2}}^{\frac{\beta}{2}} d\tau_1 d\tau_2 d\tau_3 \langle \tilde{J}_1^z \tilde{J}_2^z \tilde{\mathcal{O}}_3^{(i)} \rangle_{T,c} \\ & + \frac{1}{2\beta} \sum_{i=c,s,f} \lambda_i \lambda_j \int \int_{-\infty}^{\infty} dx_1 dx_2 \int \dots \int_{-\frac{\beta}{2}}^{\frac{\beta}{2}} d\tau_1 \dots d\tau_4 \langle \tilde{J}_1^z \tilde{J}_2^z \tilde{\mathcal{O}}_3^{(i)} \tilde{\mathcal{O}}_4^{(j)} \rangle_{T,c} + \text{subleading terms}, \quad (62) \end{aligned}$$

where $\mathcal{O}^{(c)} = J, J^z \equiv J_s^z, J_i^z \equiv J^z(\tau_i, x_i), \mathcal{O}_k^{(i)} \equiv \mathcal{O}^{(i)}(\tau_k, 0)$ and $\mathcal{O}^{(s,f)} = \mathbf{J}_{-1}^{(s,f)} \cdot \phi^{(s,f)}$. Note that there is no term to zeroth order in λ_i , for the same reason that zeroth order terms were absent in the expansion of the impurity specific heat. Terms linear in λ_c and λ_f are easily seen to vanish in (62) due to charge-, spin-, and

flavor decomposition of correlation functions: $\langle \mathcal{O}^{(c)} \rangle$ and $\langle \mathcal{O}^{(f)} \rangle$ factor out, and with these operators being Virasoro primaries, the expectation values vanish. Writing out the remaining connected three-point function in the spin sector (going back to the complex plane for notational simplicity), we have

$$\langle J_1^z J_2^z \mathcal{O}_3^{(s)} \rangle_c = \langle J_1^z J_2^z \mathcal{O}_3^{(s)} \rangle - \langle J_1^z J_2^z \rangle \langle \mathcal{O}_3^{(s)} \rangle - \langle J_1^z \mathcal{O}_3^{(s)} \rangle \langle J_2^z \rangle - \langle J_2^z \mathcal{O}_3^{(s)} \rangle \langle J_1^z \rangle - \langle J_1^z \rangle \langle J_2^z \rangle \langle \mathcal{O}_3^{(s)} \rangle, \quad (63)$$

with $J_k^z \equiv J^z(z_k)$ and $\mathcal{O}_k^{(s)} = \mathcal{O}^{(s)}(z_k)$. Again, all terms in Eq. (63) containing one-point functions are zero since J^z and $\mathcal{O}^{(s)}$ are Virasoro primaries. Then, inserting the operator product expansions⁵⁰

$$J^z(z_1)\mathcal{O}^{(s)}(z_2) = \frac{3}{(z_1 - z_2)^2}\phi^{(s)z}(z_2) + \text{regular terms in } (z_1 - z_2), \quad (64)$$

$$J^z(z_1)\phi^{(s)z}(z_2) = \text{regular terms in } (z_1 - z_2), \quad (65)$$

into $\langle J_1^z J_2^z \mathcal{O}_3^{(s)} \rangle$, this three-point function collapses⁵¹ to a sum of vanishing one-point functions in the neighborhood of $z_1 \sim z_2 \sim z_3$. Since the three-point functions in Eq. (63), $\langle J_1^z J_2^z \mathcal{O}_3^{(s)} \rangle_c$ and $\langle J_1^z J_2^z \mathcal{O}_3^{(s)} \rangle$, both vanish for infinite separations of the fields, analyticity then implies

that $\langle J_1^z J_2^z \mathcal{O}_3^{(s)} \rangle_c = 0$ for any z_1, z_2, z_3 . One concludes that there is no contribution to χ_{imp} linear in λ_s .

Turning to the terms in Eq. (62) quadratic in the scaling fields, we have (again going back to the complex plane)

$$\begin{aligned} \langle J_1^z J_2^z \mathcal{O}_3^{(i)} \mathcal{O}_4^{(i)} \rangle_c &= \langle J_1^z J_2^z \mathcal{O}_3^{(i)} \mathcal{O}_4^{(i)} \rangle - \langle J_1^z J_2^z \rangle \langle \mathcal{O}_3^{(i)} \mathcal{O}_4^{(i)} \rangle - \langle J_1^z \mathcal{O}_3^{(i)} \rangle \langle J_2^z \mathcal{O}_4^{(i)} \rangle - \langle J_1^z \mathcal{O}_4^{(i)} \rangle \langle J_2^z \mathcal{O}_3^{(i)} \rangle - \\ &\text{-- terms containing vanishing one-point functions.} \end{aligned} \quad (66)$$

As for the case above and as expected on physical grounds, only terms containing the spin boundary operator $\mathcal{O}^{(s)}$ can potentially contribute in Eq. (66). Injecting Eq. (64) into $\langle J_1^z \mathcal{O}_3^{(s)} \rangle \langle J_2^z \mathcal{O}_4^{(s)} \rangle$ and $\langle J_1^z \mathcal{O}_4^{(s)} \rangle \langle J_2^z \mathcal{O}_3^{(s)} \rangle$, these terms are seen to vanish, and one is left with

$$\langle J_1^z J_2^z \mathcal{O}_3^{(s)} \mathcal{O}_4^{(s)} \rangle - \langle J_1^z J_2^z \rangle \langle \mathcal{O}_3^{(s)} \mathcal{O}_4^{(s)} \rangle. \quad (67)$$

The four-point function in Eq. (67) is easily calculated, again by exploiting the operator product expansions in Eqs. (64) and (65). Transforming to the finite- T geometry Γ_c , one finds:⁵¹

$$\begin{aligned} \langle \tilde{J}^z(\tau_1, x_1) \tilde{J}^z(\tau_2, x_2) \tilde{\mathcal{O}}^{(s)}(\tau_3, 0) \tilde{\mathcal{O}}^{(s)}(\tau_4, 0) \rangle_{T,c} &= \\ &= 9 \left[h(\tau_1 - \tau_3 + ix_1) h(\tau_2 - \tau_4 + ix_2) + h(\tau_2 - \tau_3 + ix_2) h(\tau_1 - \tau_4 + ix_1) \right] \left| \frac{\beta}{\pi} \sin \frac{\pi}{\beta} (\tau_3 - \tau_4) \right|^{-1}, \end{aligned} \quad (68)$$

where $h(z) \equiv [(\beta/\pi) \sin(\pi z/\beta)]^{-2}$. Inserting Eq. (68) into (62) and carrying out the integration, one finally obtains, to $O(\lambda_s^2)$ [with all other terms in Eq. (62) vanishing to this order]:

$$\chi_{imp} = 18\lambda_s^2 \ln\left(\frac{T_s}{T}\right) + O(\lambda_s^3), \quad (69)$$

where we have subtracted a temperature-independent nonuniversal constant (what in practice fixes the scale T_s). Using the Bethe Ansatz result for T_s and λ_s that we give in the next section, we finally obtain a complete determination of the asymptotic low-temperature behavior of the susceptibility.

Notice that for the case of the response to an external field in the flavor degrees of freedom the calculations proceed in a completely analogous way and the final result

is the same with the obvious replacements $T_s \rightarrow T_f$ and $\lambda_s \rightarrow \lambda_f$.

D. Numerical Fit

We can use the numerical solution of the TBA equations in Ref. 17 to find the values of the conjugate scaling fields and temperature scales that parametrize the line of boundary conformal fixed points. This is, to our knowledge, the first time that this kind of fit is being explicitly carried out.

We start from the following asymptotic expression for the free energy from which the above results for the entropy, specific heat, and susceptibilities follow immediately:

$$F_{\text{imp}}[\{t, h_{s,f} \ll t\}] = F_{\text{imp}}^0 - T S_{\text{imp}}^0 + \sum_{x=s,f} \frac{(3\pi\lambda_x)^2}{2} T^2 \ln \frac{T}{T_x} \left(1 + \frac{2h_x^2}{\pi^2 T^2} \right) + O(\{T^2, h_{s,f}^3\}) \quad (70)$$

with $F_{\text{imp}}^0 = \text{const}$, $S_{\text{imp}}^0 = k_B \ln \sqrt{2}$, and $h_{s,f}$ the external field acting on the spin or flavor degree of freedom respectively. In order to carry out the fit, we define the quantities

$$\tilde{\chi}_{\text{imp}}^x \equiv \frac{2}{h_x^2} (F_{\text{imp}}[\{T, h_x \ll T, h_{\bar{x}} = 0\}] - F_{\text{imp}}[\{T, h_{s,f} = 0\}]) = 18\lambda_x^2 \ln \frac{T}{T_x} + O(\{T^2, h_{s,f}^3\},) \quad (71)$$

which coincide with minus the field susceptibilities in their low- T behavior and deviate from them as the temperature increases. We have here used the notation $\bar{x} = s(f)$ if $x = f(s)$. The advantage of these quantities over the usual susceptibilities is that they incorporate the knowledge that we have about the form that the leading free energy terms take and they are numerically simpler to compute.

We fitted the data from the numerical solution of the TBA equations in the appropriate temperature range using the form $\tilde{\chi}_{\text{imp}}^x = \tilde{a}_x \ln T + \tilde{b}_x$ and extracted the desired parameters (as functions of ε): $\lambda_x = \frac{1}{3} \sqrt{\frac{\tilde{a}_x}{2}}$ and $\ln T_x = -\frac{\tilde{b}_x}{\tilde{a}_x}$. We also computed $B_x = \lambda_x \sqrt{T_x}$. In Fig. 1 we show the values obtained for λ_f as a function of the doublets energy difference ε (we have taken $\mu = 0$).

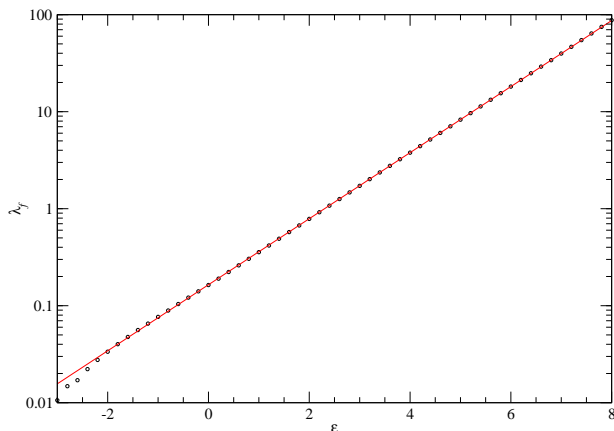


FIG. 1: The dots are the Thermodynamic Bethe Ansatz numerical results for the flavor scaling field as a function of ε (both in units of Γ) and the line is our exponential fit.

In the same figure we show a fit using the function $\lambda_f = \lambda_0 e^{\gamma\varepsilon}$ that gives the values: $\lambda_0 = 0.1640 \pm 0.0004$ and $\gamma = 0.7838 \pm 0.0004$. The fit was done in the interval $[-2, 8]$ and the correlation coefficient was $|R| = 0.9999935$. The errors indicated are statistical ones and do not take into account other sources of error; the total errors are somewhat larger (as we discuss below).

In Fig. 2 we show the values obtained this time for T_f as a function of the doublets energy difference. We

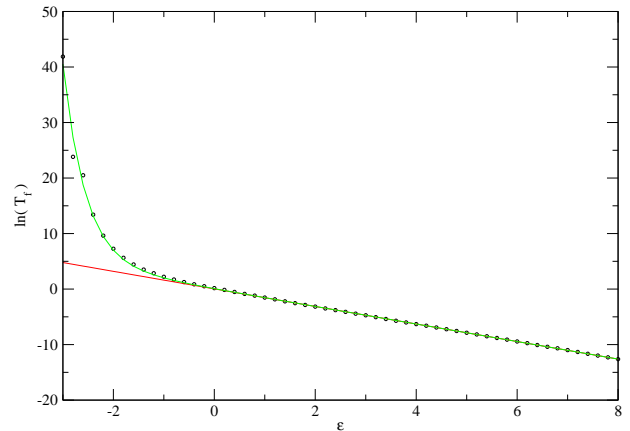


FIG. 2: The dots are the Thermodynamic Bethe Ansatz numerical results for the flavor temperature scale as a function of ε (both in units of Γ) and the lines are two different fits.

also show in the same figure the results of fitting $\ln T_f = a + b\varepsilon$ which gives the values: $a = 0.033 \pm 0.012$ and $b = -1.581 \pm 0.003$. The fit was done for $\varepsilon > 0$ and the correlation coefficient was $|R| = 0.9999501$. We next carried out the fit of a more complicated function in order to capture the behavior for $\varepsilon < 0$ as well. We fit using $\ln T_f = a + b\varepsilon + c e^{d\varepsilon}$ where a and b are taken to be those determined above. The result of this fit is also shown in the same figure, and the values obtained for the parameters were $c = 0.043$ and $d = -2.24$. The fitting was done this time in the full range of ε , with correlation coefficient $|R| = 0.998274$.

In the $\varepsilon > 0$ region, we combine the results of the two fits to obtain

$$B_f = \lambda_f \sqrt{T_f} \approx 0.1666 \approx 1/6.$$

From the expression $T_l = \frac{4\Gamma}{\pi^2} e^{-\pi/J}$ that was derived in the Bethe Ansatz analysis,¹⁷ we expect that $b = -\pi/2$ in the region where $\varepsilon \gg \Gamma$. This value is in fair agreement with the result of our fit carried out over a larger region ($\varepsilon > 0$). The agreement not only validates our results, but also serves as an indicator of the magnitude of the total errors of the numerical procedure (always necessarily larger than the statistical errors of the fit alone).

The reader should notice that the parameter a cannot be compared in a similar way since it is not a universal quantity and we did not adopt the same prescriptions in defining T_l and T_f (the prescription adopted in the latter case was that there are no constant terms in the definition of $\tilde{\chi}_{\text{imp}}^x$ and that the subleading terms are regular, i.e. vanishing, functions of the temperature).

Notice that for negative ε the scale T_f grows exponentially instead of the linear growth of the scale associated with the quenching of charge fluctuations. This is no contradiction since the two scales are not expected to be equal on physical grounds. In other words, there is no reason to expect that the leading irrelevant operator in the flavor sector will govern the charge fluctuations when $\varepsilon < 0$. One would rather expect that many operators including those in the charge sector of the theory would be involved, and in any case the quenching of charge fluctuations takes place at temperatures far removed from the domain of validity of the scaling Hamiltonian derived from BCFT. The exponential growth of T_f that we find is indicative of a very rapid suppression of the ‘importance’ of this operator relative to its counterpart in the spin sector of the theory as ε grows negative.

Finally, we also studied the effects of applying a magnetic field and confirmed numerically that

$$\begin{cases} \lambda_s(\varepsilon - \mu) = \lambda_f(\mu - \varepsilon) \\ T_s(\varepsilon - \mu) = T_f(\mu - \varepsilon) \end{cases}$$

With this observation the parameters of the asymptotic form for the free energy are now fully determined for any value of ε .

A note on some of the details of the numerical calculation is in order. The results for the free energy in the presence of an applied field were obtained using a constant field $h_{s,f} = 10^{-10}\Gamma$, which remained always at least two orders of magnitude smaller than the lower limit of the temperature range used in the fitting of $\tilde{\chi}_{\text{imp}}^{s,f}$. This was to ensure that we were always in the basin of attraction of the non-Fermi liquid fixed point and did not yet start *flowing* towards a Fermi liquid one driven by the applied field. Since we had to simultaneously capture scales that were many orders of magnitude apart ($h_{s,f}$ vs Γ) the numerical calculations had to be done using ‘quadruple precision’ arithmetics and the algorithms had to be designed carefully to assure the precision required. Let us also point out that when fitting for instance $\tilde{\chi}_{\text{imp}}^f$ for negative values of ε (i.e. determining the temperature asymptotics of the *flavor* linear susceptibility as the system goes into the overscreened *magnetic* moment regime), the quantities involved become very small and the relative errors grow rapidly.

Our results show that the infrared physics of the two-channel Anderson impurity is described by a line of non-Fermi liquid fixed points characterized by a residual entropy $S_{\text{imp}}^0 = k_B \ln \sqrt{2}$ and logarithmic temperature divergences in the specific heat coefficient (i.e.

$\gamma = C_{\text{imp}}/T$) and the susceptibilities – all these features being already present in the limiting case embodied by the two-channel Kondo impurity. What distinguishes the different points on the line are, for instance, the changing values of the impurity charge valence $n_c(\varepsilon - \mu)$ (see Fig. 3), as well as those of the scaling fields and the characteristic scales.

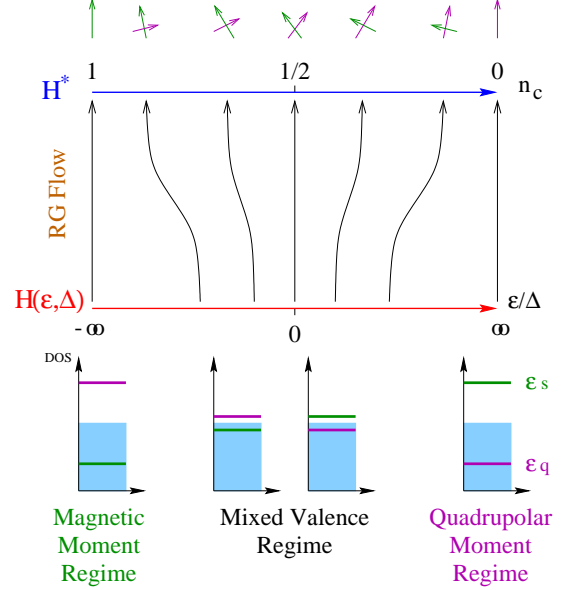


FIG. 3: Schematic renormalization group flow diagram of the two-channel Anderson impurity model. The flow connects the line of microscopic theories characterized by the ratio ε/Δ (in this figure $\Delta \equiv \Gamma$) with the line of infrared fixed points parametrized by n_c .

Since the specific heat coefficient and the susceptibilities have the same singular low-temperature divergences along the whole line of fixed points, it is possible to define the following two *Wilson ratios*:⁵²

$$R_w^{s,f} = \lim_{T \rightarrow 0} \frac{\chi_{\text{imp}}^{s,f}/\chi_{\text{bulk}}^{s,f}}{C_{\text{imp}}/C_{\text{bulk}}} \quad (72)$$

where $s(f)$ label the *magnetic (quadrupolar)* susceptibilities. This in particular gives for the ‘flavor (or quadrupolar) Wilson ratio’:

$$\begin{aligned} R_w^f(\varepsilon - \mu) &= \frac{\pi^2}{3} \lim_{T \rightarrow 0} \frac{\chi_{\text{imp}}^f}{C_{\text{imp}}/T} = \frac{8/3}{1 + (\lambda_s/\lambda_f)^2} \\ &= \frac{8/3}{1 + e^{-4\gamma(\varepsilon - \mu)}} \quad (73) \end{aligned}$$

with $\gamma = 0.7838 \pm 0.0004$. These ratios are another characteristic that varies along the line of fixed points. In particular, we have that $R_w^f(+\infty) = 8/3$ in agreement with the result for the two-channel *quadrupolar* Kondo model and, as expected, $R_w^f(-\infty) = 0$, since this is the *magnetic* Kondo limit. By symmetry arguments, we find

that $R_w^s(\varepsilon - \mu) = R_w^f(\mu - \varepsilon)$ and $R_w^f(0) = 4/3$. Finally, a simple calculation yields the universal relation: $R_w^f(\varepsilon - \mu) + R_w^s(\varepsilon - \mu) = 8/3$.

The measurement of $R_w^{s,f}$ is a very sensitive way to experimentally determine which doublet is the lower one in energy, whether the impurity ion ground state is magnetic or quadrupolar. This can be very useful if the system is in the mixed valence region $|\varepsilon - \mu| < \Gamma$, as was thought to be the case in UBe_{13} . This question triggered the interest in measuring the nonlinear susceptibility of this compound¹⁰ and its answer is still a source of some controversy.¹¹

E. Nonlinear Magnetic Susceptibility

The nonlinear magnetic susceptibility χ_3 measures the leading nonlinearity in the magnetization

$$M = \chi B + \frac{1}{6}\chi_3 B^3 + \dots \quad (74)$$

$$H_{scaling} = H^* + \lambda_s \mathcal{O}^{(s)}(0) + \lambda_f \mathcal{O}^{(f)}(0) + B \int_{-\infty}^{\infty} dx J_s^z(x) + \alpha B^2 \int_{-\infty}^{\infty} dx J_f^z(x) + \text{subleading terms}, \quad (75)$$

where we have removed ‘‘by hand’’ terms from the charge sector (which do not contribute to $\chi_{3,imp}$). Given

$$\chi_{3,imp} = -\left. \frac{\partial^4 f_{imp}}{\partial B^4} \right|_{B=0} \quad (76)$$

we now have to carry the linked cluster expansion of

$$\alpha^{\ell_0} B^4 \lambda_s^{k_0} \lambda_f^{\ell_0} \langle \Pi_{i=0,1,\dots,i_0} J_s^z(z_i) \Pi_{j=0,1,\dots,j_0} J_f^z(z_{j+i_0}) \Pi_{k=0,1,k_0} \mathcal{O}_s(z_{k+j_0+i_0}) \Pi_{\ell=0,1,\ell_0} \mathcal{O}_f(z_{\ell+k_0+j_0+i_0}) \rangle,$$

where $k_0 + \ell_0 = 1$ or 2 , and $i_0 + 2j_0 = 4$ (with $i_0 = 0, 2, 4; j_0 = 0, 2$), and where $\Pi_{m=0} \dots \equiv 1$ ($m = i, j, k, \ell$). By repeated use of the operator product expansions in Eqs. (64) and (65), a straightforward analysis reveals that among these fifteen terms only one is nonvanishing.⁵⁴ Passing to the finite- T geometry Γ_c , it has the form

$$\begin{aligned} & \langle \tilde{J}_f^z(\tau_1, x_1) \tilde{J}_f^z(\tau_2, x_2) \tilde{\mathcal{O}}^{(f)}(\tau_3, 0) \tilde{\mathcal{O}}^{(f)}(\tau_4, 0) \rangle_{T,c} \\ &= 9 \left[h(\tau_1 - \tau_3 + ix_1) h(\tau_2 - \tau_4 + ix_2) + h(\tau_2 - \tau_3 + ix_2) h(\tau_1 - \tau_4 + ix_1) \right] \left| \frac{\beta}{\pi} \sin \frac{\pi}{\beta} (\tau_3 - \tau_4) \right|^{-1}, \quad (77) \end{aligned}$$

which is the same connected four-point function that we encountered in Eq. (68), but with flavor now taking the place of spin. By comparison with the analysis that follows in Sec. (IV.C) we immediately conclude that the leading contribution to the nonlinear susceptibility has the same logarithmic form as that for the linear suscepti-

bility in the direction of an applied field B . As follows from the analysis in Ref. 53, a quadrupolar moment contributes nontrivially to χ_3 via its coupling to the square of the magnetic field. In our formalism this coupling adds a term $\alpha B^2 J_f^z$ to the scaling Hamiltonian, where α is a constant and $J_f^z = (1/2) : \psi_{\alpha\mu}^\dagger \tau_{\alpha\beta}^z \psi_{\beta\mu} :$ is the component of the quadrupolar moment along the field direction, with τ^z the diagonal $\text{SU}(2)$ flavor generator.

The fact that the quadrupolar moment couples to B^2 permits the determination of the quadrupolar susceptibility from measurements of the (nonlinear) magnetic susceptibility. Here we shall explore how the leading contribution to χ_3 from the Anderson impurity, $\chi_{3,imp}$ call it, behaves as one goes along the critical line from the quadrupolar to the magnetic two-channel Kondo fixed points.

We thus have to consider the extended scaling Hamiltonian

the free energy to $O(B^4)$, in analogy to the $O(B^2)$ expansion in the calculation of the linear susceptibility in Sec. (IV.C). To second order in the scaling fields λ_s and λ_f we then find that f_{imp} can receive possible contributions from 15 different terms generated by $H_{scaling}$ in Eq. (75). These terms have the structure

bility, but now parametrized by the ‘‘quadrupolar’’ scaling field λ_f and temperature scale T_f :

$$\chi_{3,imp} = 18 \lambda_f^2 \alpha^2 \ln\left(\frac{T_f}{T}\right) + O(\lambda_f^3). \quad (78)$$

Combined with the Bethe Ansatz fit of λ_f and T_f from

the previous section, Eq. (78) completely specifies the leading scaling term of the nonlinear magnetic susceptibility.

V. SUMMARY

We have carried out in this paper a detailed analysis of the low-temperature thermodynamics of the two-channel Anderson impurity model, identifying and fitting a boundary conformal field theory to the Bethe Ansatz solution of the model. Combining the methods allowed us to completely determine the various parameters and scales introduced in the BCFT and, in terms of these, give a complete description of the line of fixed points characterizing the low-energy physics.

As we mentioned in the Introduction, having identified the scaling operators the asymptotic dynamical properties can in principle be calculated. This allows the study of resistivities, optical conductivities, and Green's functions in general. These results will be presented in a subsequent work.

Acknowledgments

This work was started while one of us (H. J.) was visiting Rutgers University. He thanks the Physics Department for its hospitality, and the Swedish Research Council and the STINT foundation for financial support. We are grateful to P. Coleman and P. Fonseca for useful and enlightening discussions.

* Present address at Université de Genève, Switzerland.

- ¹ For a modern perspective on Landau theory, see R. Shankar, *Rev. Mod. Phys.* **66**, 129 (1994).
- ² See, e.g., R. W. Hill, C. Proust, L. Taillefer, P. Fournier, and R. L. Greene, *Nature* **414**, 711 (2001).
- ³ M. Bockrath, D. H. Cobden, J. Lu, A. G. Rinzler, R. E. Smalley, T. Balents, and P. L. McEuen, *Nature* **397**, 598 (1999).
- ⁴ For a review, see C. Bourbonnais and D. Jerome, in *Advances in Synthetic Metals*, edited by P. Bernier, S. Lefrant, and G. Bidan (Elsevier, New York, 1999).
- ⁵ O. M. Auslaender, A. Yacoby, R. de Picciotto, K. W. Baldwin, L. N. Pfeiffer, and K. W. West, *Science* **295**, 825 (2002).
- ⁶ G. R. Stewart, *Rev. Mod. Phys.* **73**, 797 (2001).
- ⁷ H. R. Ott, H. Rudigier, Z. Fisk, and J. L. Smith, *Phys. Rev. Lett.* **50**, 1595 (1983).
- ⁸ D. L. Cox, *Phys. Rev. Lett.* **59**, 1240 (1987).
- ⁹ B. Andraka and A. M. Tsvelik, *Phys. Rev. Lett.* **67**, 2886 (1991).
- ¹⁰ A. P. Ramirez, P. Chandra, P. Coleman, Z. Fisk, J. L. Smith, and H. R. Ott, *Phys. Rev. Lett.* **73**, 3018 (1994).
- ¹¹ F. G. Aliev, H. El Mfarrej, S. Vieira, R. Villar, and J. L. Martinez, *Europhys. Lett.* **32**, 765 (1995).
- ¹² F. G. Aliev, S. Vieira, H. P. van der Meulen, K. Bakker, and A. V. Andreev, *JETP Lett.* **58**, 762 (1993).
- ¹³ For a review, see D. L. Cox and A. Zawadowski, *Adv. Phys.* **47**, 599 (1998).
- ¹⁴ A. Schiller, F. B. Anders and D. L. Cox, *Phys. Rev. Lett.* **81**, 3235 (1998).
- ¹⁵ J. Kroha and P. Wölfle, *Act. Phys. Pol. B* **29**, 3781 (1998).
- ¹⁶ N. Andrei, K. Furuya and J. H. Lowenstein, *Rev. Mod. Phys.* **55**, 331 (1983).
- ¹⁷ C. J. Bolech and N. Andrei, *Phys. Rev. Lett.* **88**, 237206 (2002).
- ¹⁸ I. Affleck, *Nucl. Phys. B* **336**, 517 (1990).
- ¹⁹ I. Affleck and A. W. W. Ludwig, *Nucl. Phys. B* **360**, 641 (1991).
- ²⁰ For a review, see I. Affleck, *Acta Phys. Pol.* **26**, 1869 (1995).
- ²¹ A. W. W. Ludwig, in *Proceedings of the Fourth Trieste Conference on Quantum Field Theory and Condensed*

Matter Physics, edited by S. Randjbar-Daemi and L. Yu (World Scientific, Singapore, 1994).

- ²² H. Saleur, *Proceedings of the 1998 Les Houches Summer School*, cond-mat/9812110.
- ²³ J. L. Cardy, *J. Phys. A* **17**, L385 (1984)
- ²⁴ P. Di Francesco, P. Mathieu, and D. Senechal, *Conformal Field Theory* (Springer-Verlag, New York, 1997).
- ²⁵ For a review, see C. Itzykson and J.-M. Drouffe, *Statistical Field Theory*, Vol 2 (Cambridge University Press, Cambridge, 1989).
- ²⁶ J. L. Cardy, *Nucl. Phys. B* **240**, 512 (1984); *ibid.* **324**, 581 (1989).
- ²⁷ H. J. de Vega and F. Woynarovich, *Nucl. Phys. B* **251**, 439 (1985).
- ²⁸ A. Hewson, *The Kondo Problem to Heavy Fermions*, (Cambridge University Press, Cambridge, England, 1993).
- ²⁹ P. W. Anderson, *Phys. Rev.* **124**, 41 (1961).
- ³⁰ S. Fujimoto, N. Kawakami and S.-K. Yang, *Phys. Rev. B* **50**, 1046 (1994).
- ³¹ P. B. Wiegmann, *Phys. Lett.* **80A**, 163 (1980).
- ³² D. C. Langreth, *Phys. Rev.* **150**, 516 (1966).
- ³³ P. Nozières and J. Blandin, *J. Phys. (Paris)* **41**, 193 (1980).
- ³⁴ S. Fujimoto and N. Kawakami, *Phys. Rev. B* **52**, R13102 (1995).
- ³⁵ N. Andrei and C. Destri, *Phys. Rev. Lett.* **52**, 364 (1984).
- ³⁶ A. M. Tsvelik and P. B. Wiegmann, *Z. Phys. B* **54**, 201 (1984).
- ³⁷ G. E. Andrews, R. J. Baxter, and P. J. Forrester, *J. Stat. Phys.* **35**, 193 (1984).
- ³⁸ Note that while the lattice physics underlying the Kondo model is not expected to respect charge conjugation symmetry, the Kondo model itself is invariant under the corresponding transformation $\psi_\sigma(x) \rightarrow \epsilon_{\sigma\mu} \psi_\mu^\dagger(x)$. The reason for this is that the normal ordering of the electron fields in the model subtracts the symmetry-breaking terms. We may remove this accidental symmetry by explicitly introducing operators that break charge conjugation, of which the leading one is the charge current $J(0)$. However, in the case of the Kondo model there is no tunable parameter that can change its conjugate scaling field λ_c [in contrast to the Anderson model considered here where $\lambda_c = \lambda_c(\epsilon_s, \epsilon_q) = -n_c(\epsilon_s, \epsilon_q)/4$ (cf. Eq. (23)]. For this rea-

- son the marginal charge current plays no role in the Kondo model other than generating trivial subleading corrections to the leading impurity critical behavior.¹⁹
- ³⁹ B. Menge and E. Müller-Hartmann, *Z. Phys. B* **73**, 225 (1988).
- ⁴⁰ T. A. Costi, P. Schmitteckert, J. Kroha, and P. Wölfle, *Phys. Rev. Lett.* **73**, 1275 (1994).
- ⁴¹ See S. Fujimoto, N. Kawakami, and S.-K. Yang, *J. Phys. Soc. Jpn.*, **64**, 4552 (1995), and references therein.
- ⁴² P. Nozières and C. T. de Dominicis, *Phys. Rev.* **178**, 1097 (1969).
- ⁴³ E. Müller-Hartmann, T. V. Ramakrishnan, and G. Toulouse, *Phys. Rev. B* **3**, 1102 (1971).
- ⁴⁴ I. Affleck and A. W. W. Ludwig, *J. Phys. A* **27**, 5375 (1994).
- ⁴⁵ H. Johannesson, N. Andrei, and C. J. Bolech, unpublished.
- ⁴⁶ D. L. Cox and A. E. Ruckenstein, *Phys. Rev. Lett.* **71**, 1613 (1993).
- ⁴⁷ I. Affleck and A. W. W. Ludwig, *Phys. Rev. Lett.* **67**, 161 (1991).
- ⁴⁸ J. Cardy, *Scaling and Renormalization in Statistical Physics* (Cambridge University Press, Cambridge, England, 1997).
- ⁴⁹ P. Fröjdh and H. Johannesson, *Phys. Rev. B* **53**, 3211 (1996).
- ⁵⁰ V. G. Knizhnik and A. B. Zamolodchikov, *Nucl. Phys. B* **247**, 83 (1984).
- ⁵¹ For details, see Appendix C in Ref. 19.
- ⁵² K. G. Wilson, *Rev. Mod. Phys.* **47**, 773 (1975).
- ⁵³ K. R. Lea, M. J. Leask, and W. P. Wolf, *J. Phys. Chem. Solids* **23**, 1381 (1962).
- ⁵⁴ By inspection one also verifies that there is no contribution to $O(B^2)$ coming from the coupling of the magnetic field to the quadrupolar moment. Hence, the result derived in Sec. (IV.C) for the *linear* susceptibility remains valid also when this coupling is included in the scaling Hamiltonian.